Response to Reviewer 1

RC1-1: The authors should be more clear about motivation for their study. Simulations described in the manuscript cannot contribute to understanding of the mechanisms of glacial termination since GHGs and ice sheets were prescribed. Their experiments also do not represent true transient simulations and cannot be compared with rich archive of continuous climate records which reveals strong millennial-scale variability. Even for the LGM and mid-Holocene simulations their model set-up is not realistic because the model does not account for the effects of vegetation cover change and aeolian dust. The later was not even mentioned in the manuscript. At the same time, there is a significant body of modeling studies (e.g. Mahowald et al. 2006, Takemura et al., 2009; Crucifix and Hewitt, 2005; Schneider von Deimling et al., 2006; O'ishi and A. Abe-Ouchi, 2013) which clearly indicate that climate effects of dust and vegetation are comparable (1-2C additional cooling) to the effect of ice sheets and GHGs. Even comparison with other models (PMIP 2 and 3) is limited by the fact that the authors used different ice sheet reconstruction.

We agree that the purpose and motivation for our study were not clearly articulated. We have added the following sentences to the end of the introduction to improve clarity about the motivation and scope of the study:

"The goal of our simulations is to adopt a methodological framework similar to that of PMIP and extend the time slices beyond the LGM and mid-Holocene. The simulations also serve as a base line for applying GENMOM to more detailed and focused studies of late-Pleistocene climate such as freshwater forcing and dynamic vegetation."

We disagree that our simulations do not contribute to our understanding of glacial and deglacial climate because they are not transient. While they do not include mechanisms such as freshwater forcing, they do provide multi-century time series that are useful, for example, to explore ecosystem responses to changes in mean climate and the related interannual variability in the model. As we show below, our simulations are also in good agreement with several transient simulations.

Our experimental design follows PMIP which includes non-interactive vegetation and fixed atmospheric aerosols. Similar boundary conditions were used in the transient simulations analyzed by Liu et al. (2014). We recognize that feedbacks from changes in vegetation and aerosol loading have been demonstrated to play a role in LGM and deglacial climate simulations (Mahowald et al., 2006). Not addressing the potential added effect of radiative forcing by aerosols was our oversight. We point out, however, that the global distribution of LGM aerosols is not well constrained and that estimated dust concentrations fall by over an order of magnitude between the LGM and 16 ka, and reach mean concentrations similar to PI by 14 ka (Harrison and Bartlein,

2012) which would reduce their contribution to cooling over their time slices substantially. Aerosol loading associated with volcanism is increasingly being viewed as a potential source of lower magnitude Holocene climate variability. We have revised our text to mention the lack of aerosol forcing in our simulations and potential radiative impact of aerosols. We will be modifying GENMOM in the future in order to assimilate aerosol loading and dynamic vegetation.

The ICE6G reconstruction used in PMIP3 provides more realistic ice sheet topography than the previous ICE5G. Currently, the ICE6G reconstruction is not available for our 8 time slices. However, the OSU-LIS reconstruction has similar ice sheet topography to that of ICE6G (Ullman et al., 2014) and is available for our simulation periods. The combination of OSULIS+ICE4G enabled us to use a more realistic LIS topography than that of ICE5G, particularly for the deglacial, and facilitated adjusting sea level throughout our time slides. Future work assessing the atmospheric circulation, storm tracks and the mass balance over the LIS will test GENMOM's sensitivity to different ice sheet configurations (ICE4G+OSULIS, ICE5G and ICE6G).

RC1-2: When comparing with paleoclimate data one have to be aware about limitations of paleoclimate reconstructions which by no means are "observations". For example direct comparison of global modeled SAT with Shakun et al. (2012) "global" temperature reconstruction is meaningless. Shakun's reconstruction at best represents "global" SAT anomalies outside of the NH continental ice sheets. At the same time, the latter through albedo and orographic effects, are responsible for additional cooling of at least 2C (e.g.Schneider von Deimling et al., 2006; Singarayer and Valdes, 2010; Hargreaves et al., 2012). The authors apparently try to address this inconsistency at the page 2935 but what they want to say here is unclear to me.

That our comparison is meaningless is perhaps an overstatement. Nevertheless, we appreciate the criticism and have accordingly revised the figure and section extensively. Figure 5 now displays a) our original figure to which we have added output from the three transient simulations in Liu et al. (2014) and b) the Shaken et al. (2012) and Marcott et al. (2013) data and GENMOM, the PMIP3 models and the three transient simulations averaged over 5° × 5° boxes around the core sites. The cores are predominantly coastal SST records away from the ice sheets, so sampling the models at these sites provides a more direct comparison. The addition of the transient models also puts the GENMOM changes into context for periods other than the LGM and mid-Holocene. We mention the possibility issue for seasonal biases in the reconstructions raised by Liu et al. (2014), but we do not explore the topic further.

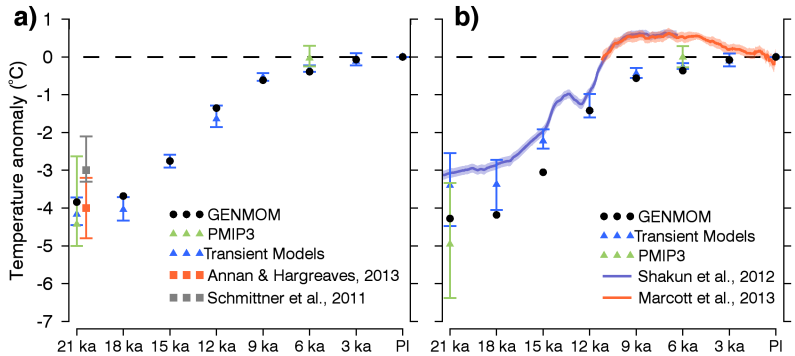

Figure 5 (revised). a) Mean-annual global air temperature anomalies, b) mean-annual temperature anomalies sampled at the core locations. Transient model mean-annual model temperatures calculated over 50-yr windows centered on the indicated times. (Full figure caption in revised manuscript text.)

RC1-3: Even more problematic is comparison with MARGO SST in the tropics. Systematic disagreement between foraminiferal-based reconstructions and other proxies (Mg/Ca, alkenones, elevation change of snow line, terrestrial data) as well as similar systematic differences between MARGO and PMIP modeling results in the Pacific and Indian oceans cast serious doubts on reliability of MARGO reconstructions in the tropics. This is why it is rather strange that, when discussing tropical SST at the LGM, the authors compare their results only with MARGO but not with PMIP modeling results. In fact, most of PMIP models simulate considerably stronger cooling in the tropics compare to GENMOM.

We are aware of potential issues with the MARGO dataset; however, the MARGO (and GHOST) data have been, and continue to be, used to evaluate model-based changes in SSTs (Harrison et al., 2013). Recent work has shown that both modern observations and models do not capture long-term SST variability displayed in proxy records (Laepple and Huybers, 2014). It is beyond the scope of this paper to go into the details and caveats of each paleo reconstruction. GENMOM is warmer than the mean of the PMIP2 models in these basins; it was not our intent to obscure that fact. The GENMOM SST anomalies fall within the maximum-minimum range of the six PMIP2 models. Moreover, on a global scale, our mean LGM SST anomaly of 2.42 °C is essentially the same as that for the ensemble of all PMIP2 and PMIP3 models (Harrison et al., 2013). We have modified the text accordingly.

RC1-4: Some important aspects of methodology are missing. In particular, what was the fate of snow accumulated over the ice sheets? Was it added to freshwater flux into the ocean and, if yes, were? What surface type was prescribed for the land grid cells which at present are covered by ocean? It is also unclear why the authors used old ICE-4G reconstruction for the ice sheets instead of more recent one.

As we discuss in Alder et al (2011), excess freshwater over land, including snow melt from the ice sheets, is totaled globally and the flux is computed as the average over the world ocean. (Similar to most models, meltwater from prescribed ice sheets is not included in the hydrologic balance.) We have modified the text to clarify.

The vegetation types for emergent land cells are prescribed from neighboring land cells. We have modified the text to clarify.

We addressed the choice ice sheet reconstructions above.

Specific comments
p. 2926, l. 24. What is the meaning of "unforced"? Obviously this AMOC change was "forced" by changes in prescribed boundary conditions.

We originally intended this to allude to the absence of N. Atlantic freshwater forcing in our simulations but we now see that it adds unnecessary confusion. The word unforced was removed from the text.

p. 2927 l. 8/9. It is unclear from the text whether "global warming" is caused only by GHGs or also to NH summer insolation. Since the latter cannot cause global warming, I would recommend to reformulate this sentence.

We revised the sentence:

"The effect of the ice sheets on climate progressively diminished from the LGM to the early Holocene as global warming driven by increasing GHGs combined with changes in NH summer insolation to accelerate ice sheet ablation."

p. 2928, l. 14. what is the difference between "time segment" and commonly used "time slice"?

Our simulations are 1100-yr long and the related time series of post-spin-up output span several centuries; however, in keeping with the standard naming conventions, we have replaced "segments" with "slices."

p. 2928, l. 17. Does "time-appropriate" means that orbital parameters were kept constant during each individual run?

Yes, the orbital parameters are held constant over each 1100 time slice simulation. We removed he phrase "time-appropriate" from the text.

P.2935,l. 2/3"SLP anomalies...are negative due to lower presser..."Sounds like tautology.

We have revised the sentence.

p. 2936 "...warm winter and summer temperature changes..." sounds odd. I would suggest to change "warm" to "positive".

We have revised the sentence.

p. 2936, l 20-24. It is unclear what is the link between global temperature and seasonality of insolations. It is known that precession and obliquity do not affect global insolation and have rather small direct impact on global temperature. Of course, in the real world insolation affects ice sheets but in the current study ice sheets are prescribed.

We did not intend to imply that changes in insolation timing drive changes in global temperature. We moved the sentence in question to the proceeding paragraph.

p. 2938, l. 28. "may have altered" is rather strange formulation for modeling paper. Altered or not?

Altered. We have revised the text.

p. 2939, l. 5,6. "The NH summer monsoons are suppressed globally". The meaning is unclear

This section has been revised and moved two paragraphs down to the discussion of the North African and Indian monsoons, which it was intended to refer to.

p. 2941, l. 24. "simulated sea-ice fraction". Firstly, the authors discuss sea ice area, not fraction. Secondly, in fact sea ice area in the NH is increasing (not decreasing) from LGM to Holocene because of increasing Arctic ocean area.

This sentence was removed and the section rearranged to address comments from both Reviewer 1 and Reviewer 2.

p. 2942, l. 8,9. "The model captures the spatial distribution of more sea ice...". Please reformulate.

We rearranged the sentence:

"The model displays increased sea ice in the western North Atlantic and decreased ice in the eastern North Atlantic and Nordic Seas where the prescribed FIS margin advances into the water (Fig. 2)"

p. 2943 , l. 25. IPCC AR5 report is now available. Please cite it instead of AR4.

The text now includes values for both CMIP3 (max AMOC) and CMIP5 (AMOC@30N).

Response to Reviewer 2

p.2928 line 20-23: this part of the text could be moved into the previous paragraph, together with the rest of the PMIP model simulation descriptions (add in line 4).

We have moved the text as suggested.

Methods:
p.2930: line 15-16: It is unclear what is meant with 'permanent sea ice': 'perennial sea ice'?

The 'permanent' was indeed meant to be perennial, we have revised the sentence.

p.2930: Question: was the doubling CO2 sensitivity estimated from a present-day climate state?

It is interesting to see that despite the lower climate sensitivity the LGM to Holocene temperature trend is in the same order of magnitude as the reconstructions suggest (see my later comment in under the Summary Section).

Yes, the 2xCO2 experiment used to establish sensitivity was relative a present-day simulation.

p. 2930: line 27: Unclear what 'which' stands for the PD or PI temperature: '[. . .], which is 1.97 C cooler than observations [. . .]'. Only afterwards it becomes clear that it must be the PD simulation.

We have rearranged the sentence to clarify we are referring to the PD simulation.

p.2930: last paragraph and p.2931 first paragraph: What does it mean that the NH temperature trend is of the right magnitude compared with observations, if the model has a low climate sensitivity in the CO2 doubling experiment?

The PD -> 2xCO_2 sensitivity of 2.2 °C implies that the 75 ppm PI -> PD change in CO_2 which is ~1/4 of the doubling, would result in ~0.55 °C change from CO_2 alone. In addition to CO_2, we changed CH_4 concentration by a factor of ~2.25 between PI and PD simulations, which would also contribute to the net warming of 0.79 °C. Quantifying the radiative contributions of CO_2 and CH_4 individually in GENMOM would require an additional set of targeted model runs, which is beyond our focus here.

p. 2932: paragraph 1: One could consider adding Renssen et al., GRL, (2005), Notaro et al, GRL, (2006) to the references.

We have added a citation to the Renssen et al. paper.

p.2932-2933, last paragraph: It is okay to choose one calendar definition over the other, however, are the insolation curves in Figure 1, the mid-month values of Berger and Loutre (1991), or are these the also now fixed-calendar seasonal averages? This issue should be resolved in the Figure 1 caption. (See also Chen et al., Clim. Dyn. (2010)).

The insolation curves in Fig. 1 are mid-month values from Berger and Loutre (1991). The caption has been updated with this information.

Results:
p.2934: line 21-23: It is unclear what is the location and direction component of the pressure gradient? North-South gradient towards the equator or towards the Mediterranean?

This sentence was an editing artifact from a previous version that belonged in an expanded monsoon section. Similar text is already in the monsoon section so we removed the sentence.

p.2934: last paragraph (line 25 +): Does he difference pattern also suggests a slight north-south shift in the pressure systems (in particular together with the later discussed rainfall it could make sense)?

The Aleutian low is expanded southward and the center of the Icelandic low is shifted to the southeast. We have revised the text with the appropriate description.

Section 3.2
p. 2935 l.10-28: The recent paper by Liu et al. in PNAS (2014) should be taken into account in discussing the differences in the global mean temperature trends of the Holocene.

The Liu et al. (2014) paper was published after our submission. We cite and draw from that paper in our revision. See discussion of Reviewer 1 Comments.

p.2936 l.12: south of the FIS: by that is meant the region which extends into the central Asian continent, right?

Yes, we revised the text to clarify this point

p.2936 l. 24: write 'precessional shift of perihelion, and by changes in obliquity'

We have revised the text as suggested.

p.2937 l. 17: Please start the new sentence with the season '[. . .] warming over America. During summer, GENMOM simulates [. . .] consistent with [. . .]'

We have rearranged the sentence.

Section 3.3:
page 2938: l. 10-14: This is an example where the compression of complex information is dangerous. What is seen in precipitation anomalies in the model is associated through a 'short-cut' chain of causal relations. How certain is it that the described 'quasi-global' precipitation pattern is caused only by the ice-sheet /sea-ice changes and not through tropical SST changes in response to orbital and GHG forcing (locally)?

We have rewritten this section to be more spatially focused and to indicate positive anomalies in precipitation along the Gulf of Mexico and Eastern US are driven by changes in circulation, as reflected in z500 anomalies.

p.2941 last paragraph: It should be made clear in the beginning that NH sea ice area extent is controlled by bathymetry (land-sea-area changes). Area changes are in response to external forcing are thus biased.

We have clarified the bathymetric controls at the beginning of the paragraph.

p.2942 first paragraph l. 4-5: It would be better to write 'not affected by land-sea area changes with global sea level rise' (in this model at least; ice-shelf changes could indeed change the ocean area for sea ice)

We have revised the text accordingly.

p.2944 first paragraph: Please take into consideration the recent study by Marson et al, Clim. Past, (2014) (doi:201410.5194/cp-10-1723-2014)

In earlier versions of the AMOC section of our manuscript we included a detailed description of changes in AABW in our simulations based on the evaluation of the PMIP models by Weber et al. (2007), but we removed the discussion for brevity. It may not be appropriate to compare the GENMOM changes in water masses to those discussed in Marson et al, due to the lack of a freshwater forcing in our experimental design.

Section 4.2
p.2946: line 25-26: I am confused by the use of the word 'regionally coherent pattern' and 'contrasting areas of warming'. Is a coherent pattern a pattern with only positive (or negative) anomalies, whereas 'contrasting areas' show both positive and negative anomalies? Could it be labeled as 'regionally incoherent pattern'? Or does the use of words suggest an inconsistency with a reference pattern (e.g. the pattern reconstructed by proxies)?

This was sentence was ambiguous. We have revised it.

Section 5: Summary:
p.2948 l.21-27: Climate sensitivity was found to be on the low end for doubling CO2. If the LGM cooling is now consistent and in the middle range of the estimated LGM cooling, I wonder would that indicate a higher climate sensitivity during the LGM (a result suggesting a 'state-dependent' climate sensitivity?) or is it suggesting that the cooling contribution from ice-sheets (here an external forcing) is overestimated / or proxies may underestimate the global cooling contribution (e.g. they may not sample appropriately the NH ice-sheet regions). Or is the climate sensitivity and LGM cooling altogether consistent within the margin of uncertainties?

The climate sensitivity of GENMOM to a doubling of CO_2 ***is similar to previous studies using GENESIS and a mixed layer ocean. A lower sensitivity paired with a middle of the range LGM estimate could indicate a strong ice-albedo or other fast feedbacks in the model. Ullman et al., (2014) showed that uncertainties in the LIS topography could produce different global temperatures, and hence, drive uncertainties in the inferred paleo sensitivity. It should also be noted our LGM simulation lowers the concentration of*** CH_4 ***by nearly half that of PI, which could play a significant radiative roll. We have not performed the additional modeling simulations to quantify GENMOM's sensitivity to*** CH_4***. The proxy stack from Shaken et al. very likely does not capture 'global' temperature with 80 sites that are predominantly coastal marine records. Our analyses indicate it is unclear if the proxy sites under or over estimate temperature change at the LGM. We feel GENMOM has a reasonable sensitivity and LGM cooling given the uncertainties in the proxies, imperfect sampling and good agreement with results of similar models.***

<u>References</u>:

Harrison, S. P., P. J. Bartlein, S. Brewer, I. C. Prentice, M. Boyd, I. Hessler, K. Holmgren, K. Izumi, and K. Willis (2013), Climate model benchmarking with glacial and mid-Holocene climates, Clim Dyn.

Laepple, T., and P. Huybers (2014), Ocean surface temperature variability: Large model-data differences at decadal and longer periods, P Natl Acad Sci USA, 111(47), 16682-16687.

Liu, Z. Y., J. Zhu, Y. Rosenthal, X. Zhang, B. L. Otto-Bliesner, A. Timmermann, R. S. Smith, G. Lohmann, W. P. Zheng, and O. E. Timm (2014), The Holocene temperature conundrum, P Natl Acad Sci USA, 111(34), E3501-E3505.

Ullman, D. J., A. N. LeGrande, A. E. Carlson, F. S. Anslow, and J. M. Licciardi (2014), Assessing the impact of Laurentide Ice Sheet topography on glacial climate, Clim Past, 10(2), 487-507.

Global climate simulations at 3,000-year intervals for the last 21,000 years with the GENMOM coupled atmosphere-ocean model

J. R. Alder and S. W. Hostetler

Jay R. Alder, US Geological Survey, College of Earth, Ocean and Atmospheric Sciences, Oregon State University, Corvallis, Oregon 97331, United States, jalder@usgs.gov

Steven W. Hostetler, US Geological Survey, College of Earth, Ocean and Atmospheric Sciences, Oregon State University, Corvallis, Oregon 97331, United States, swhostet@usgs.gov

Corresponding author address: Jay Alder
E-mail: jalder@usgs.gov

Abstract

We apply GENMOM, a coupled atmosphere-ocean climate model, to simulate eight equilibrium time slices at 3000-yr intervals for the past 21,000 years forced by changes in Earth-Sun geometry, atmospheric greenhouse gases (GHGs), continental ice sheets and sea level. Simulated global cooling during the Last Glacial Maximum (LGM) is 3.8 °C and the rate of post-glacial warming is in overall agreement with recently published temperature reconstructions. The greatest rate of warming occurs between 15 and 12 ka (2.4 °C over land, 0.7 °C over oceans and 1.4 °C globally) in response to changes in radiative forcing from the diminished extent of the Northern Hemisphere (NH) ice sheets and increases in GHGs and NH summer insolation. The modeled LGM and 6 ka temperature and precipitation climatologies are generally consistent with proxy reconstructions, the PMIP2 and PMIP3 simulations, and other paleoclimate data-model analyses. The model does not capture the mid-Holocene 'thermal maximum' and gradual cooling to pre-industrial global temperature found in the data. Simulated monsoonal precipitation in North Africa peaks between 12 and 9 ka at values ~50% greater than those of the PI, and Indian monsoonal precipitation peaks at 12 and 9 ka at values ~45% greater than the PI. GENMOM captures the reconstructed LGM extent of NH and Southern Hemisphere (SH) sea ice. The simulated present-day Antarctica Circumpolar Current (ACC) is ~48% weaker than the observed (62 versus 119 Sv). The simulated present-day Atlantic Meridional Overturning Circulation (AMOC) of 19.3 ± 1.4 Sv on the Bermuda Rise (33°N) is comparable with observed value of 18.7 ± 4.8 Sv. AMOC at 33°N is reduced by ~15% during the LGM, and the largest post-glacial increase (~11%) occurs during the 15 ka time slice.

Steve 1/15/15 2:34 PM
Deleted: "

Jay Alder 12/8/14 1:46 PM
Deleted: -segments

Steve 1/15/15 2:34 PM
Deleted: "

Jay Alder 12/15/14 4:17 PM
Deleted:

Jay Alder 12/15/14 4:17 PM
Deleted: 17.4

Jay Alder 12/28/14 9:24 AM
Comment: R1: What is the meaning of "unforced"? Obviously this AMOC change was "forced" by changes in prescribed boundary conditions.

Jay Alder 12/8/14 2:28 PM
Deleted: , unforced,

1 Introduction

The history of the climate system over the past 21,000 years reflects the combined changes in earth-sun orbital geometry, atmospheric greenhouse gas concentrations (GHG), the extent of the Northern Hemisphere (NH) ice sheets, and sea level. GHG levels were lowest during the Last Glacial Maximum (LGM, ~21,000 years ago, 21 ka) and increased thereafter to pre-industrial (PI) levels (Brook et al., 2000; Monnin et al., 2001; Sowers et al., 2003). The LGM is further characterized by the large Laurentide (LIS), Cordilleran (CIS) and Fennoscandian (FIS) ice sheets. The height and extent of the ice sheets altered atmospheric circulation patterns, and the extent increased the NH albedo thereby altering the global radiative balance. The effect of the ice sheets on climate progressively diminished from the LGM to the early Holocene as global warming driven by increasing GHGs combined with changes in NH summer insolation to accelerate ice sheet ablation. Abrupt departures from the comparatively smooth transition from the LGM through the Holocene, such as Heinrich and Dansgaard-Oeschger events, the Bølling-Allerød (BA), and the Youger Dryas (YD), are evident in geologic records, and these events likely influenced the overall trajectory of the deglaciation.

The climate of the past 21,000 years has been studied extensively, beginning with three international collaborative projects: the Long range Investigation, Mapping, and Prediction (CLIMAP; CLIMAP Project Members, 1981) and the Cooperative Holocene Mapping Project (COHMAP; COHMAP Members, 1988), which evolved into the Testing Earth System Models with Paleoenvironmental Observations (TEMPO) project (Kutzbach et al., 1996a; 1998). CLIMAP focused on reconstructing the LGM climate, COHMAP focused on reconstructing the climate of seven time periods (18, 15, 12, 9, 6, 3

Jay Alder 12/28/14 9:24 AM
Comment: R1: It is unclear from the text whether “global warming” is caused only by GHGs or also to NH summer insolation. Since the latter cannot cause global warming, I would recommend to reformulate this sentence.

Jay Alder 12/8/14 2:43 PM
Deleted: and

Jay Alder 12/8/14 2:45 PM
Deleted: accelerat

Jay Alder 12/8/14 2:44 PM
Deleted: ed

Jay Alder 12/8/14 2:44 PM
Deleted: their

ka), and TEMPO focused on reconstructing the climate of 21, 16, 14, 11 and 6 ka. These three projects pioneered data-model comparison through integrating climate model simulations and paleoclimatic data, which motivated the development of new techniques for analyzing geologic data and led to improvements in general circulation models.

More recently, the Palaeoclimate Modelling Intercomparison Project (PMIP) is actively working to advance reconstruction of LGM and 6 ka climate through model-to-model evaluations and data-model comparisons. PMIP has now entered the third phase (PMIP3; Braconnot et al., 2012) and is a component of phase 5 of the Climate Model Intercomparison Project (CMIP5). In contrast to CLIMAP, COHMAP, TEMPO and earlier PMIP model experiments that employed fixed sea surface temperatures (SST) and mixed-layer ocean models, some of the PMIP2 experiments and all of the PMIP3 experiments include fully coupled ocean and atmospheric models. Braconnot et al. (2012) review some of the highlights of the PMIP2 experiments and the design of the PMIP3 experiments and Harrison et al. (2013) evaluate the PMIP3 and PMIP2 simulations of LGM and 6 ka climates with data-model comparisons. In addition, continuous simulations of climate over the last 21 ka have been achieved with earth system models of intermediate complexity (e.g., Timm and Timmermann, 2007), and the TraCE-21ka project at the National Center for Atmospheric Research (NCAR) conducted continuous, transient climate simulations from 22 ka to 6.5 ka with the coupled NCAR Community Climate System Model (Liu et al., 2009). Singarayer and Valdes (2010) simulated the climate of the last 120,000 years using model snapshots at 4 ka and 1 ka intervals.

Jay Alder 12/17/14 2:54 PM
Deleted:

Steve 1/16/15 9:23 AM
Deleted: and data, while

Jay Alder 12/28/14 9:24 AM
Comment: R2: add text below here

Here we explore past changes in late-Pleistocene climate using the coupled Atmosphere-Ocean General Circulation Model (AOGCM) GENMOM. We simulated multi-century time slices that span the interval from LGM to pre-industrial (PI) every three thousand years (21, 18, 15, 12, 9, 6, 3 ka and PI). The simulations were run with prescribed insolation, GHG concentrations, continental ice sheets, land extent and sea level as boundary conditions. We analyze the within and between climatology of the time slices and compare the 21 ka and 6 ka results with terrestrial and marine climate reconstructions and results from the PMIP2 and PMIP3 simulations. The goal of our simulations is to adopt a methodological framework similar to that of PMIP to simulate time slices between the LGM and mid-Holocene. The simulations also serve as a base line for applying GENMOM to more detailed and focused studies of late-Pleistocene climate such as quantifying the effects of freshwater forcing and dynamic vegetation feedbacks.

2 Methods

2.1 Model description

GENMOM combines version 3 of the GENESIS atmospheric model (Pollard and Thompson, 1997; Thompson and Pollard, 1995; 1997) with version 2 of the Modular Ocean Model (MOM2, Pacanowski, 1996). Version 3 of GENESIS (Alder et al., 2011; Kump and Pollard, 2008; Pollard and Thompson, 1997; Zhou et al., 2008) incorporates the NCAR CCM3 radiation code (Kiehl et al., 1998). GENESIS has been developed with an emphasis on representing terrestrial physical and biophysical processes, and for application to paleoclimate experiments. Earlier versions of GENESIS (Pollard and Thompson, 1994; 1995; 1997; Thompson and Pollard, 1995; 1997) have been applied in

Jay Alder 12/28/14 9:24 AM
Comment: R1: what is the difference between "time segment" and commonly used "time slice"?
Steve 1/15/15 2:35 PM
Deleted: "
Jay Alder 12/8/14 1:46 PM
Deleted: segments
Steve 1/15/15 2:36 PM
Deleted: "
Jay Alder 12/28/14 9:24 AM
Comment: R1: Does "time-appropriate" means that orbital parameters were kept constant during each individual run?
Jay Alder 12/10/14 2:55 PM
Deleted: and time-appropriate
Jay Alder 12/8/14 1:46 PM
Deleted: segments
Jay Alder 12/28/14 9:24 AM
Comment: R2: this part of the text could be moved into the previous paragraph, together with the rest of the PMIP model simulation descriptions
Jay Alder 12/8/14 5:02 PM
Deleted: Braconnot et al. (2012) review some of the highlights of the PMIP2 experiments and the design of the PMIP3 experiments and data and Harrison et al. (2013) evaluate the PMIP3 and PMIP2 simulations of LGM and 6 ka climates with data-model comparisons.
Jay Alder 12/28/14 9:18 AM
Deleted:
Steve 1/16/15 9:23 AM
Deleted: and extend
Steve 1/16/15 9:24 AM
Deleted: the
Steve 1/16/15 9:24 AM
Deleted: beyond
Jay Alder 12/28/14 9:18 AM
Deleted:

a wide range of modern and paleoclimate studies (Beckmann et al., 2005; Bice et al., 2006; DeConto et al., 2007; 2008; Horton et al., 2007; Hostetler et al., 2006; Miller et al., 2005; Poulsen et al., 2007a; 2007b; Ruddiman et al., 2005; Tabor et al., 2014), and GENESIS simulations with fixed and slab ocean SSTs were included in PMIP1 (Joussaume et al., 1999; Pinot et al., 1999; Pollard et al., 1998).

In our simulations, we employ a coupled model with T31 spectral truncation, which corresponds to a grid of 96 longitudes (3.75°) by 48 Gaussian latitudes (~3.71°). The atmosphere is represented by 18 vertical sigma levels with mid-layers ranging from 0.993 at the surface to 0.005 at the tropopause. GENESIS includes the Land Surface eXchange model, LSX, (Pollard and Thompson, 1995) to simulate surface processes and to account for the exchange of energy, mass and momentum between the land surface and the atmospheric boundary layer. MOM2 has 20 fixed-depth vertical levels and is implemented on essentially the same T31 horizontal grid as GENESIS through cosine-weighted distortion (Pacanowski, 1996). Sea ice is simulated by a three-layer model that accounts for local melting, freezing, and fractional cover (Harvey, 1988; Semtner, 1976) and includes the dynamics associated with wind and ocean current using the cavitating-fluid model of Flato and Hibler (1992). The atmospheric and ocean models interact every six hours without flux corrections.

GENMOM reproduces observed global circulation patterns, such as the seasonal change in the position and strength of the jetstreams and the major semi-permanent sea level pressure centers (Alder et al., 2011). The simulated present-day (PD) 2-m air temperature climatology (Table 1) is 0.8 ºC colder than observations globally, 0.7 ºC colder over oceans, and 0.9 ºC colder over land. Similar to other AOGCMs (e.g., Lee and Wang, 2012), GENMOM produces a split ITCZ over the equatorial Pacific Ocean.

The pre-industrial Atlantic Meridional Overturning Circulation (AMOC) simulated by GENMOM is 19.3 ± 1.4 Sv, which is stronger than, but comparable to, the observed value of 17.4 Sv (Srokosz et al., 2012). Simulated SSTs display a warm bias in some regions of the Southern Ocean, primarily south of 50ºS around Antarctica, and a warm bias exceeding ~2 ºC between 200–1000 m depth in parts of the tropics and mid-latitudes. Alder et al. (2011) note that the warm bias in the Southern Ocean is associated with the relatively weak Antarctic Circumpolar Current (ACC) in GENMOM (62 Sv versus the observed value of 119 Sv) and Deacon Cell upwelling which allows excessive vertical mixing in the present-day GENMOM simulation, and together reduce sea ice around Antarctica, particularly during summer. Both of these features are present to some extent in our suite of simulations. We tested the Gent-McWilliams vertical ocean mixing scheme (Gent and McWilliams, 1990) in GENMOM but it did not improve the Southern Ocean warm bias, so we did not implement it in our paleosimulations.

The climate sensitivity of GENMOM for a doubling of CO_2 from present day is 2.2 ºC, which is in the lower range of other coupled AOGCMs (Meehl et al., 2007) and is consistent with recent estimates of 2.7 ºC based on the PMIP3 LGM simulations (Harrison et al., 2013) and paleodata-model estimates of 2.8 ºC (Annan and Hargreaves, 2013) and 2.3 ºC (Schmittner et al., 2011b).

Reflecting lower GHG concentrations, the average NH 2-m temperature in our PI simulation is 0.79 °C cooler than our PD simulation, where as the PD simulation is 1.97 ºC cooler than observations and reflects the lower GHG concentrations specified in the PI

Jay Alder 12/28/14 9:24 AM
Comment: R2: It is unclear what is meant with 'permanent sea ice': 'perennial sea ice'?

Jay Alder 11/18/14 4:17 PM
Deleted: which,

Jay Alder 11/18/14 4:17 PM
Deleted: s

Jay Alder 12/11/14 10:31 AM
Deleted: permanent

Jay Alder 11/18/14 4:17 PM
Deleted: ocean

Jay Alder 11/18/14 4:18 PM
Deleted: and

Jay Alder 12/28/14 9:24 AM
Comment: R2: Question: was the doubling CO2 sensitivity estimated from a present-day climate state?

It is interesting to see that despite the lower climate sensitivity the LGM to Holocene temperature trend is in the same order of magnitude as the reconstructions suggest (see my later comment in under the Summary Section).

Jay Alder 12/11/14 11:22 AM
Deleted: The

Jay Alder 12/28/14 9:24 AM
Comment: R2: Unclear what 'which' stands for the PD or PI temperature: '[. . .], which is 1.97 C cooler than observations [. . .]'. Only afterwards it becomes clear that it must be the PD simulation.

Jay Alder 12/11/14 11:19 AM
Deleted: which

simulation (Tables 1 and 2). The PI-to-PD warming in the NH is similar to the observed warming of ~0.6 – 0.9 °C (Brohan et al., 2006) and is in the range of response of other climate models (e.g., Otto-Bliesner et al., 2006b). The greatest regional warming between the in the PD simulation (not shown) is ~3 °C over the high northern latitudes and northern polar regions during boreal autumn, winter and spring, consistent with the observed polar amplification (Hassol, 2004).

2.2 Experimental design

We applied GENMOM to eight time periods for 21, 18, 15, 12, 9, 6, 3 ka and pre-industrial. We prescribed insolation at the top of atmosphere for each time slice (Fig. 1) by specifying appropriate orbital parameter values for precession, obliquity and eccentricity (Table 1, Berger and Loutre, 1991). The solar constant was set to 1367 W m^{-2} for all time periods. We estimated GHG concentrations from ice-core records by applying a ±300 yr averaging window centered on the time period of interest (Table 1), and we specified the PMIP3 GHG concentrations for our PI simulation (Braconnot et al., 2007a).

To derive continental ice sheets for the time slices, we used the ICE-4G reconstructions (Peltier, 2002) for the Fennoscandian (FIS) and Cordilleran (CIS), and the Oregon State University Laurentide Ice Sheet (OSU-LIS) reconstruction (Hostetler et al., 1999; Licciardi et al., 1998) (Fig. 2). The ICE-6G reconstruction was not available for our 8 time slices at time we began our simulations. However, the OSU-LIS reconstruction has similar ice sheet topography to that of ICE-6G {Ullman:2014hg} and is available for our simulation periods. The combination of OSU-LIS and ICE-4G enables us to use a more realistic LIS topography than that of ICE-5G, particularly over the LIS during the deglacial, and facilitates adjusting sea level throughout our time slices.

Jay Alder 12/28/14 9:24 AM
Comment: R2: What does it mean that the NH temperature trend is of the right magnitude compared with observations, if the model has a low climate sensitivity in the CO2 doubling experiment?

Jay Alder 12/8/14 1:46 PM
Deleted: segment

Jay Alder 12/8/14 1:47 PM
Deleted: segments

Steve 1/15/15 2:39 PM
Deleted: The ICE-6G reconstruction used in PMIP3 provides more realistic ice sheet topography than the previous ICE-5G. Currently, t

Jay Alder 1/16/15 3:47 PM
Deleted: currently

Jay Alder 1/16/15 3:48 PM
Deleted:

Steve 1/15/15 2:51 PM
Deleted: for

A similar ice sheet configuration (OSU-LIS and ICE5-G) was used as a boundary condition in the NASA GISS-E2-R LGM simulation submitted to the PMIP3 archive {Ullman:2014hg}. We specified the 10 ka OSU-LIS ice sheet to ensure that Hudson Bay remained covered by the LIS at 9 ka (Dyke and Prest, 1987). The ICE-4G reconstruction includes an Eastern Siberian Ice Sheet, which we removed because it did not exist (Felzer, 2001).

Topographic heights of the land masses were altered to reflect relative sea-level change in ICE-4G. We created the topography and land mask for each time slice by applying orographic changes to the present-day Scripps global orography data set (Gates and Nelson, 1975). Orographic changes based on ICE-4G exposed or flooded land grid cells associated with relative sea level (e.g. Indonesia, Papua New Guinea). We set the ocean bathymetry to modern depths for ocean grid cells.

Jay Alder 12/8/14 1:47 PM
Deleted: segment

We specified the modern distribution of vegetation (Dorman and Sellers, 1989) for all simulations because reconstructions of global vegetation for all time slices either do not exist or are not well constrained. We note that while setting vegetation to modern distribution for all simulations isolates the period-to-period climate response to other boundary conditions, we do not capture dynamic vegetation-climate feedbacks that may be important in some regions such as North Africa (Kutzbach et al., 1996b; Timm et al., 2010) and the high latitudes of the NH {Claussen:2009gi, Renssen:2004iq}. The vegetation type on emergent land cells is set to be the same as neighboring existing land cells. The simulations do not include varying dust forcing across the time slices, which may account for up to 20% of the radiative change {Kohler:2010ux, Rohling:2012ey}.

Jay Alder 12/8/14 1:47 PM
Deleted: segments

Jay Alder 12/28/14 9:24 AM
Comment: R2: One could consider adding Renssen et al., GRL, (2005), Notaro et al, GRL, (2006) to the references.

Freshwater flux from land-based precipitation is globally averaged and spread over the world ocean {Alder:2011ki}.

In accordance with the PMIP3 protocol, to conserve atmospheric mass we compensated for changes in global topography in each time slice by holding global average surface pressure constant. At T31 resolution the Bering Strait and the Strait of Gibraltar are closed in the default MOM2 bathymetry. We conducted sensitivity tests and adjusted the bathymetry to ensure that key passages (e.g. Drake Passage, Norwegian Sea, and Indonesian Throughflow) were adequately represented. Additional sensitivity testing revealed that the modeled AMOC and salinity of the Arctic are very sensitive to the bathymetry of the Norwegian Sea, particularly to the width of the passage between Scandinavia and Greenland as it narrowed by the growth of the FIS. We removed Iceland from the model to ensure that the passage remained sufficiently wide and deep to prevent unrealistic buildup of salinity in the Arctic.

Each time slice simulation was initialized from a cold start (isothermal atmosphere, latitudinally dependent ocean temperature profile, and uniform salinity of 35 ppt) and run for 1,100 years. We exclude the first 1,000 years from our analysis here to allow for spin up of ocean temperatures. The temperature drift in the last 300 years of our simulations (SFig. 1) is acceptably small (Braconnot et al., 2007a; Singarayer and Valdes, 2010) with values of -0.05 ºC/century for the LGM, 0.01 ºC/century for 6 ka, and -0.02 ºC/century for PI. Drift in the LGM and early deglacial simulation is attributed primarily to long-term cooling and the evolution of sea ice in the southern ocean. Simulated AMOC exhibits decadal scale variability, but was free of drift over the last 300 years of the simulations.

Jay Alder 12/8/14 1:47 PM
Deleted: segment

Jay Alder 12/8/14 1:47 PM
Deleted: -

Jay Alder 12/8/14 1:47 PM
Deleted: segment

In what follows, the monthly averages of the model output are based on the modern calendar as opposed to the angular calendar that changes with Earth-sun geometry (Pollard and Reusch, 2002; Timm et al., 2008). The modern calendar is commonly used in data-model comparisons (e.g., Harrison, 2013).

Jay Alder 12/28/14 9:24 AM
Comment: R2: It is okay to choose one calendar definition over the other, however, are the insolation curves in Figure 1, the mid-month values of Berger and Loutre (1991), or are these the also now fixed-calendar seasonal averages? This issue should be resolved in the Figure 1 caption. (See also Chen et al., Clim. Dyn. (2010)).

3 Results

3.1 Atmospheric circulation

The boreal winter (DFJ) 500 hPa heights in the PI simulation (Fig. 3a) display the observed high- and mid-latitude ridge-trough-ridge-trough standing wave structure (wave number two) that arises from continent-ocean-continent-ocean geography of the NH (Peixoto and Oort, 1992). From 21 ka to 9 ka the LIS, the FIS and Greenland ice sheets alter the NH standing wave structure resulting in persistent, distinct troughs and cyclonic flow tendencies over northeast Asia, the North Pacific, the continental interior of North America, the North Atlantic and Europe (Fig. 3, maps of raw fields SFig. 2).

Consistent with previous LGM studies using comparable (Braconnot et al., 2007a) and higher-resolution (Kim et al., 2007; Unterman et al., 2011) climate models, from 21 ka through 9 ka the western edge of the Cordilleran Ice Sheet diverts the LGM winter polar jetstream resulting in one branch that is weaker than PI over the Gulf of Alaska and the western and central regions of the ice sheet, and a second branch to the south of the ice sheet that is stronger than the PI (Fig. 3a). The reorganization creates westward wind anomalies over the North American Pacific Northwest. The LIS effectively guides the convergence of the branches, and the meridional gradient of low and high 500 hPa height anomalies in the North Atlantic intensifies flow over North America, the North Atlantic, Europe and Northern Africa (Figs. 3a) thereby altering the path of storm tracks. This flow pattern weakens progressively as the LIS recedes.

The influence of the NH ice sheets is also evident in summer (JJA), but to a lesser degree than in winter (Fig. 3b) due to continental heating and the absence of the strong, mid-latitude storm tracks. Between 21 ka and 15 ka, the summer jetstream is constrained and therefore enhanced along and to the south of the southern margin of the LIS extending over the North Atlantic. At 18 ka, a trend toward positive JJA anomalies in 500 hPa heights emerges over the regions of the semi-permanent subtropical high pressure of the North Pacific and central Atlantic. The regions of positive height anomalies, and their associated anticyclonic wind anomalies, expand over central North America, peak from 12 ka through 9 ka, and diminish by 6 ka (Fig. 3). The DJF pattern of low-to-high height anomalies over the North Atlantic is replaced during JJA by a strengthened subtropical high. Anticyclonic flow around positive height anomalies on the western edge of the FIS alters regional flow patterns over and south of the ice sheet. The GENMOM responses to the NH ice sheets are similar to many previous modeling experiments that have established that changes in tropospheric pressure–surface heights and winds are primarily driven by changes in ice-sheet height, and secondarily by temperature and albedo feedbacks (COHMAP Members, 1988; Felzer et al., 1996; 1998; Otto-Bliesner et al., 2006a; Pausata et al., 2011; Pollard and Thompson, 1997; Rind, 1987).

From 21 ka to 12 ka, the largest changes in boreal winter sea-level pressure (SLP) are associated with negative surface temperature anomalies over the continental ice sheets, the landmasses of the NH, and areas of expanded sea ice in the North Atlantic (Fig. 4a) where cooling increases subsidence and thus contributes to cold high surface pressure. From 21 ka to 15 ka, high pressure over the LIS produces anticyclonic flow across the northern Great Plains and over the Puget Lowlands of the US. Similar anticyclonic tendencies are simulated along the margin of the FIS. Between 12 ka and 6 ka the winter SLP around the Aleutian low in the North Pacific and the Icelandic low in the North Atlantic is strengthened relative to PI. The Aleutian low is expanded southward whereas the Icelandic low is confined on the northern edge by the FIS and is slightly displaced southeastward.

From 21 ka to 9 ka, the JJA SLP anomalies remain strongly positive over the ice sheets and sea ice, whereas from 12 ka to 6 ka the SLP anomalies over Northern Hemisphere landmasses are negative due to enhanced continental warming (Fig. 4b). The patterns of the JJA 500 hPa heights, SLP and the associated circulation over North America and adjacent oceans again illustrate similar responses to time-varying controls: changes from 21 ka to 15 ka are primarily driven by changes in the LIS, whereas from 12 ka to 6 ka the circulation changes are related to the changes in the seasonality of Holocene NH insolation (Fig. 2).

3.2 Near-surface air temperature

Our time slice simulations clearly display surface air temperature (SAT) changes attributed to radiative forcing from the presence of the continental ice sheets, GHGs (Clark et al., 2012), and insolation (Fig. 5). The global average mean annual LGM temperature simulated by GENMOM is 3.8 °C colder than the PI (Table 2, Fig. 5a), within the range of cooling in the PMIP2 AOGCM simulations (3.1 °C to 5.6 °C and average 4.4 °C) and the PMIP3 simulations (2.6 °C to 5.0 °C and average of 4.4 °C) that were forced by similar boundary conditions (Harrison et al., 2013; Kageyama et al.,

Jay Alder 12/28/14 9:24 AM
Comment: R2: It is unclear what is the location and direction component of the pressure gradient? North-South gradient towards the equator or towards the Mediterranean?

Jay Alder 12/12/14 10:19 AM
Deleted: Between 21 and 12 ka, changes in the surface-pressure gradient over Africa and the Indian subcontinent reflect a transition in the location and strength of the Hadley circulation as the NH ice sheets melt and global temperature increases, whereas the mid-to-late Holocene changes are the result of changes in the seasonality of insolation and related continental heating and land-sea temperature contrasts.

Jay Alder 12/28/14 9:24 AM
Comment: R2: Does he difference pattern also suggests a slight north-south shift in the pressure systems (in particular together with the later discussed rainfall it could make sense)?

Jay Alder 12/12/14 10:23 AM
Deleted:

Jay Alder 12/28/14 9:24 AM
Comment: R1: SLPanomalies…arenegativeduetolowerpresser…"Soundslike tautology.

Jay Alder 12/12/14 10:52 AM
Deleted: lower pressure associated with

Jay Alder 12/8/14 1:47 PM
Deleted: -segment

2006). Our LGM cooling is also in agreement with Annan and Hargreaves (2013), who reconciled the PMIP2 ensemble and proxy data to derive an estimated cooling of 4.0 ± 0.8 °C, but falls outside the range of Schmittner et al. (2011b) who found a median cooling of 3.0 ºC (66% probability range of 2.1 ºC - 3.3 ºC). GENMOM is also consistent with three transient simulations {Liu:2014bc} averaged over the periods simulated by GENMOM. Excluding the BA and YD, our simulations reproduce the rate of warming between 21 ka and 15 ka, but are consistently ~1 °C colder than the reconstruction of Shakun et al. (2012) when sampled at the proxy sites (Fig. 5b). During these periods, GENMOM falls at the low end or outside the range of the transient models; however, GENMOM falls within the range of LGM and MH cooling simulated by the PMIP3 models, which have similar experimental designs and large scale boundary conditions.

Neither GENMOM nor the ensemble mean of the PMIP3 models capture the ~0.5 °C the 6 ka temperature anomaly in the Marcott et al. (2013) reconstruction. The change in the 6 ka mean annual temperature at the proxy sites in the 12 PMIP3 models we analyzed ranged from -0.3 to 0.3 °C with a mean of ~0.0 °C. Three models simulated slight warming, five near zero and four simulated slight cooling. Whether or not some proxies used in the temperature reconstructions have seasonal bias which would exaggerate the mid-Holocene warming remains an open research question {Liu:2014bc}.

Seasonal temperature changes across our time slice simulations illustrate the spatial and temporal effect of changing boundary conditions (Fig. 6). From 21 ka through 15 ka, both DJF and JJA exhibit cold temperature anomalies exceeding 16 °C over and adjacent to the ice sheets in both hemispheres. With the exception of Europe and the high latitudes of the NH, boreal winters remain generally colder than PI over the continents

Steve 1/16/15 8:13 AM
Deleted: The…LGM …that …LGM …also compares well to ... [1]

Jay Alder 1/16/15 4:19 PM
Deleted: LIU et al, 2014

Steve 1/15/15 2:54 PM
Deleted: when their temporal resolution is degraded to…In almost every time slice, the global cooling simulated by GENMOM falls within the range of the three transient models. the ... [2]

Jay Alder 12/12/14 12:20 PM
Deleted: 12 …0.5 – 0.75…, likely reflecting cooling over the continental ice sheets that is included in the model average. During the Holocene, between 12 ka and 9 ka our simulations do not reproduce the warming in the Marcott et al. (2013) reconstruction, nor do they capture the gradual cooling trend from the mid-Holocene to PI. ... [3]

Steve 1/16/15 8:16 AM
Deleted: is on…. H…is…wide …an … similar to our own ... [4]

Jay Alder 12/12/14 2:19 PM
Deleted: The global average mean annual LGM temperature simulated by GENMOM is 3.8 °C colder than the PI (Table 2, Fig. 5), within the range of cooling in the PMIP2 AOGCM simulations (3.1 to 5.6 and average 4.4 °C) and the PMIP3 simulations (2.6 to 4.9 and average of 4.4 °C) that were forced by similar boundary conditions (Harrison et al., 2013; Kageyama et al., 2006). The LGM cooling is also in agreement with Annan and Hargreaves (2013), who reconciled the PMIP2 ensemble and proxy data to derive an estimated LGM cooling of 4.0 ± 0.8 °C, but falls outside the range of Schmittner et al. (2011b) who found that a median LGM cooling of 3.0 ºC (66% probability range of 2.1 ºC - 3.3 ºC).

Steve 1/16/15 8:18 AM
Deleted: 5 …at 6 ka ... [5]

Jay Alder 12/12/14 2:43 PM
Deleted: global …1 …Six … (average of 0.1 °C) six … (average of -0.1 °C) ... [6]

Jay Alder 12/28/14 9:24 AM
Comment: R2: The recent paper by Liu et al. in PNAS (2014) should be taken into account in discussing the differences in the global mean temperature trends of the Holocene.

Steve 1/16/15 8:21 AM
Deleted: It should be noted that it is currently an open research question if …types of …a …rather than recording mean annual temperature, …- ... [7]

Jay Alder 12/12/14 2:51 PM
Deleted:

Jay Alder 12/8/14 1:47 PM
Deleted: -segment

until 3 ka (Fig. 6), corresponding to reduced insolation. NH atmospheric circulation changes induced by atmospheric blocking from the LIS (Fig. 3) sustain positive winter and summer temperature anomalies over Beringia. Summer warming also occurs south of the FIS across much of Asia. Although the mid-Holocene wintertime deficit in insolation is small at high northern latitudes, changes in short-wave radiation at the surface during boreal summer in the model are large and positive (30 – 40 Wm^{-2}) due to the precessional shift of perihelion and changes in obliquity (SFig. 4). Substantial warming occurs between most pairs of consecutive time slices from the LGM through the Holocene (Fig. 7, Table 2); however, over the African and Indian monsoon regions increased cloudiness associated with enhanced summer monsoonal precipitation leads to cooling from 15 to 6 ka.

The relatively high rate of warming between 18 ka and 15 ka (1.5 °C land and 0.5 °C ocean, Fig. 7, Table 2) is commensurate with increased GHGs (Table 1). Periods of peak annual warming from 15 ka to 12 ka (2.4 °C land and 0.7 °C ocean) and from 12 ka to 9 ka (1.6 °C land and 0.2 °C ocean) are associated with increasing GHG concentrations, ablation of the NH ice sheets (Figs. 1 and 6a). The simulated rates of annual global warming between the LGM and the early Holocene (Fig. 5) are in agreement with data (Clark et al., 2012; Gasse, 2000), and the analyses by Shakun et al. (2012) and Marcott et al. (2013) who attribute a large component of the warming to rising GHG levels.

The DJF and JJA temperature differences in our 21 ka simulation are similar to those of the PMIP3, allowing for differences in between our prescribed NH ice sheets (ICE-4G+OSU-LIS in GENMOM) and the blended ice sheet of the PMIP3 simulations

Jay Alder 12/12/14 4:06 PM
Deleted: warm

Jay Alder 12/28/14 9:24 AM
Comment: R1: warm winter and summer temperature changes…" sounds odd. I would suggest to change "warm" to "positive".

Jay Alder 12/12/14 4:06 PM
Deleted: changes

Jay Alder 12/28/14 9:24 AM
Comment: R2: by that is meant the region which extends into the central Asian continent, right?

Steve 1/16/15 8:22 AM
Deleted: the summertime surface

Jay Alder 12/28/14 9:24 AM
Comment: R1: It is unclear what is the link between global temperature and seasonal- ity of insolations. It is known that precession and obliquity do not affect global insolation and have rather small direct impact on global temperature. Of course, in the real world insolation affects ice sheets but in the current study ice sheets are prescribed.

Steve 1/16/15 8:22 AM
Deleted: changes

Jay Alder 12/28/14 9:24 AM
Comment: R2: write 'precessional shift of perihelion, and by changes in obliquity'

Jay Alder 12/8/14 1:48 PM
Deleted: segments

Steve 1/16/15 8:25 AM
Deleted: 5

Jay Alder 12/28/14 9:24 AM
Comment: R1: It is unclear what is the link between global temperature and seasonal- ity of insolations. It is known that precession and obliquity do not affect global insolation and have rather small direct impact on global temperature. Of course, in the real world insolation affects ice sheets but in the current study ice sheets are prescribed.

Jay Alder 12/28/14 9:24 AM
Comment: R2: write 'precessional shift of perihelion, and by changes in obliquity'

Jay Alder 12/12/14 4:42 PM
Deleted: , and changes in the seasonality of NH insolation (Fig. 2, SFig. 4).

Jay Alder 12/12/14 4:43 PM
Deleted: Although the mid-Holocene wintertime deficit in insolation is small at high northern latitudes, the summertime surface short-wave radiation changes in the model are large and positive (30 – 40 Wm^{-2}) due to the precessional shift of perihelion, which is reinforced by changes in obliquity.

that essentially combines the height of the ICE6G reconstruction with the extent of the Dyke and Prest (1987) reconstructions (SFigs. 5 - 10, Braconnot et al., 2012). In both seasons, GENMOM produces 0.5 - 1 °C less cooling in the tropical oceans and greater warming over Beringia. The positive JJA temperature anomaly south of the FIS in GENMOM persists through 15 ka. Summer warming in the presence of the ice sheet was identified in earlier versions of GENESIS (Pollard and Thompson, 1997) and is associated with subsidence over the ice (Rind, 1987). Similar JJA warming also occurs in some of the PMIP3 models, but is likely a model artifact (Pollard and Thompson, 1997; Ramstein and Joussaume, 1995; Rind, 1987).

The DJF and JJA temperature anomalies in our 6 ka simulation are also similar to those of the PMIP3 models (SFigs. 7 and 8). Relative to PI, GENMOM produces slightly greater winter warming over Scandinavia than is evident in the average of the PMIP3 simulations, and is generally 0.5 - 1.0 °C cooler over Asia, Africa and South America. During boreal summer, GENMOM simulates warming over the NH landmasses and cooling over the North African and Indian monsoon regions, consistent with the PMIP3 models. Continental warming in GENMOM is ~ 0.5 - 1.0 °C weaker than most PMIP3 models, particularly in Europe and Asia. A portion of the weaker warming in GENMOM is attributed to the prescribed 6 ka GHG concentrations we derived from the ice-core data that differ slightly from those specified for the PMIP3 experiments (Table 1 caption).

3.3 Precipitation and monsoons

The simulated global precipitation anomalies display a progression from the drier and colder conditions of the LGM to the warmer and wetter conditions of the Holocene (Fig. 8, Table 2). The global mean annual precipitation change of -0.29 mm d^{-1} for the

Jay Alder 12/12/14 5:01 PM
Deleted: Consistent with the PMIP3 models

Jay Alder 12/12/14 5:01 PM
Deleted: during summer;

Jay Alder 12/12/14 5:01 PM
Deleted: although, t

Steve 1/16/15 8:27 AM
Deleted: The degree of c

Jay Alder 12/28/14 9:24 AM
Comment: R2: Please start the new sentence with the season '[. . .] warming over America. During summer, GENMOM simulates [. . .] consistent with [. . .]'

Steve 1/16/15 8:28 AM
Deleted: our

Steve 1/16/15 8:28 AM
Deleted: which

Steve 1/16/15 8:28 AM
Deleted: and

LGM is distributed as greater drying over land and ice sheets (-0.30 mm d^{-1}) than oceans (-0.22 mm d^{-1}). Regionally coherent patterns of precipitation change (Figs. 8 and 9) are indicative of displacement and changes in the strength of storm tracks (Li and Battisti, 2008), the ITCZ and the Hadley circulation, and the onset, amplification and subsequent weakening of the global monsoons regions (Broccoli et al., 2006; Chiang, 2009; Chiang and Bitz, 2005).

Between the LGM and 15 ka, during DJF areas over and adjacent to the NH ice sheets display predominately reduced precipitation arising from a combination of the desertification-effect of the high and cold ice, lower-than-present atmospheric moisture and cloudiness and the advection of cold, dry air off of the ice sheets (Figs. 3a, 4a, 6a and 8a). The topographic and thermal effects of the LIS and the thermal effect of sea ice (Kageyama et al., 1999; Li and Battisti, 2008) alter 500 hPa geopotential heights along the southern margin of the ice sheet (Figs. 3a and SFig. 2a), causing the development of positive precipitation anomalies extending from the eastern Pacific across the Gulf of Mexico, eastern North America and into the Northern Atlantic. Accompanying negative precipitation anomalies over the North Atlantic and positive anomalies over the Nordic Seas are related to changes in the location of storm tracks. The local effect of the ice sheets on precipitation diminishes during the early and mid-Holocene as their influence on circulation weakens and the atmosphere becomes warmer and moister (Fig. 9a).

The negative DJF anomalies that persist from 21 ka to 15 ka during austral summer along the equatorial and low-latitude areas of South and Central America, south-central Africa Southeast Asia, Northern Australia, the tropical Atlantic, the Indian Ocean

Jay Alder 12/15/14 1:46 PM
Deleted: and FIS

Jay Alder 12/15/14 1:42 PM
Deleted: on circulation

Jay Alder 12/15/14 1:46 PM
Deleted: combine to

Jay Alder 12/15/14 1:47 PM
Deleted: produce

Jay Alder 12/28/14 9:24 AM
Comment: R2: This is an example where the compression of complex information is dangerous. What is seen in precipitation anomalies in the model is associated through a 'short-cut' chain of causal relations. How certain is it that the described 'quasi-global' precipitation pattern is caused only by the ice-sheet /sea-ice changes and not through tropical SST changes in response to orbital and GHG forcing (locally)?

Jay Alder 1/8/15 11:58 AM
Deleted: over

Jay Alder 1/8/15 11:58 AM
Deleted: ,

Jay Alder 1/8/15 11:59 AM
Deleted: -central

Jay Alder 1/8/15 11:58 AM
Deleted: and southern Europe and Northwest Africa

and the western Pacific warm pool are caused by changes in the location of the ITCZ and weakened southern monsoonal circulation. This particularly affects the winter monsoon in central South America (Cheng et al., 2012; Zhao and Harrison, 2012) and in Southeast Asia and Indonesia where additional feedbacks in the energy and water balances over emergent land areas occur during low sea level stands (Figs. 1 and 8a) have been shown to alter the Walker Circulation (DiNezio and Tierney, 2013).

Precipitation for JJA also exhibits considerable change over time (Figs. 8b and 9b). Similar to DJF, generally drier conditions are simulated over and adjacent to the NH ice sheets where anticyclonic flow tendencies suppress precipitation (Fig. 4b). Along portions of the southern margins of the LIS and FIS, however, orographic lifting enhances precipitation at 21 ka (Pollard and Thompson, 1997). Wetter conditions in the North American Southwest derive from enhanced westerly flow aloft and lower level southwesterly flow off the eastern Pacific that are associated with displacement of the jetstream by the ice sheets and the weakened Pacific subtropical high. Between 21 ka and 12 ka the LIS causes an increased pressure gradient from a strengthened Azores-Bermuda high and weakened subtropical high in the eastern Pacific (Figs. 3b and 4b), resulting in amplified and displaced westward winds, drying over Central America, and wetter-than-present conditions over northern South America. At the LGM, North Africa, Europe, and all but the western edge of Asia, are drier than the PI, again reflecting the drier atmosphere of the full glacial.

The magnitude, gradients and spatial patterns of GENMOM 21 ka DJF precipitation anomalies are consistent with the PMIP3 experiments. Notable exceptions are greater drying than some models in the North Atlantic and the band of positive

Jay Alder 12/28/14 9:24 AM
Comment: R1: “may have altered” is rather strange formulation for modeling paper. Altered or not?

Jay Alder 12/15/14 2:06 PM
Deleted: may have

Jay Alder 12/15/14 2:06 PM
Deleted: ed

Jay Alder 12/28/14 9:24 AM
Comment: R1: “The NH summer monsoons are suppressed globally”. The meaning is unclear

Jay Alder 12/15/14 2:23 PM
Deleted: The NH summer monsoons are suppressed globally between 21 ka and 18 ka.

Jay Alder 12/15/14 2:24 PM
Deleted: After 18 ka, wetter-than-present conditions emerge in the monsoon regions of North Africa and India where increased JJA insolation warms the continents which amplifies the land-sea temperature contrasts that drive monsoonal circulation (Braconnot et al., 2007b; Kutzbach and Otto-Bliesner, 1982; Zhao and Harrison, 2012).

anomalies extending across the Gulf of Mexico and the southeast US. GENMOM produces positive precipitation anomalies over Australia, which is present in four of the PMIP3 models. The 21 ka JJA precipitation anomalies are also in agreement with PMIP3, but display weaker drying over eastern NA and slight drying over the North Africa monsoon region.

The time evolution from LGM to PI of the African and Indian monsoons reflects the interplay of changes in the location of the ITCZ and Hadley circulation that are linked to the receding NH ice sheets, GHG-driven global warming, enhanced NH JJA insolation and changing land-SST temperature contrast. The North Africa and Indian monsoons are suppressed between 21 ka and 18 ka. After 18 ka, wetter-than-present conditions emerge in the monsoon regions of North Africa and India where increased JJA insolation warms the continents which amplifies the land-sea temperature contrasts that drive monsoonal circulation (Braconnot et al., 2007b; Kutzbach and Otto-Bliesner, 1982; Zhao and Harrison, 2012). The simulated DJF air temperatures in North Africa cool from the LGM until 15 ka, and then warm monotonically through the rest of the deglaciation and Holocene (Fig. 10). Wintertime precipitation over the North African region is minimal. In contrast, JJA temperatures increase throughout the deglaciation, peak at 9 ka, decrease slightly at 6 ka, and increase thereafter. A commensurate increase in JJA precipitation over North Africa between 12 ka and 6 ka is associated with northward migration of the ITCZ (Braconnot et al., 2007a; 2007b; Kutzbach and Liu, 1997), which enhances the transport of moisture into both the North African and Indian monsoon regions. Monsoonal precipitation peaks over both regions between 12 ka and 9 ka (Fig. 10). The change in precipitation between 9 ka and 6 ka over India (0.9 mm d^{-1}) is nearly double

Jay Alder 12/28/14 9:24 AM
Comment: R1: "The NH summer monsoons are suppressed globally". The meaning is unclear

the change over North Africa (0.5 mm d^{-1}), consistent with the diagnoses of the mid-Holocene monsoon of Marzin and Braconnot (2009) who attribute the stronger ~9 ka monsoon to insolation related to precession and snow cover on the Tibetan Plateau. The pattern of precipitation in the Indian monsoon region is similar to that of North Africa, but exhibits a greater range between peak Holocene values and the PI.

The overall temporal progression and magnitude of precipitation changes in the time slice simulations are in agreement with the PMIP2 (Braconnot et al., 2007a; 2007b) and PMIP3 simulations at 21 and 6 ka, and with other mid-Holocene modeling studies (Hély et al., 2009; Kutzbach and Liu, 1997; Kutzbach and Otto-Bliesner, 1982; Timm et al., 2010). More specifically, the June through September GENMOM precipitation anomaly of -0.6 mm d^{-1} over the North Africa monsoon region during the LGM is within the range (-0.9 to 0.1 mm d^{-1}) of 5 PMIP2 AOGCMs (Braconnot et al., 2007a) and 7 PMIP3 models (range of -0.6 to 0.2 and average of -0.2 mm d^{-1}). The GENMOM LGM anomaly over India (-0.9 mm d^{-1}) is also within the range (-1.7 to -0.1 mm d^{-1}) of the PMIP2 simulations (Braconnot et al., 2007a) and the PMIP3 simulations (range of -1.3 to 0.0 and average of -0.7 mm d^{-1}).

The northward expansion and spatial pattern of precipitation anomalies of the 6 ka monsoons are in very good agreement with both the PMIP2 and PMIP3 experiments. Summer precipitation in the GENMOM simulation is enhanced by 0.9 mm d^{-1} relative to PI over North Africa, in agreement with the range (0.2 to 1.4 mm d^{-1}) and mean (0.7 mm d^{-1}) of 11 PMIP2 AOGCMs (Zhao and Harrison, 2012) and 12 PMIP3 models (range of 0.1 to 1.0 and average of 0.6 mm d^{-1}). Over India, the 6 ka GENMOM precipitation anomaly of 1.1 mm d^{-1} exceeds the range (0.2 to 0.9 mm d^{-1}) and mean (0.6

Jay Alder 12/8/14 1:48 PM
Deleted: -segment

mm d^{-1}) of the 11 PMIP2 models (Zhao and Harrison, 2012), but is within the range of the PMIP3 models (0.5 to 1.3 and average of 1.0 mm d^{-1}) .

3.4 Sea ice

DJF sea ice is present in the PI simulation over Hudson Bay, the Arctic Ocean, along the coast of eastern Canada, around Greenland, the Nordic Seas and the Baltic and North Sea (Fig. 11), in agreement with observed present-day distributions (Jaccard et al., 2005). Ice fractions of up to 100% are simulated over the Bering Sea and the Sea of Okhotsk. In the SH, sea ice persists through austral summer in the Weddell and Ross Seas and a few scattered locations around Antarctica. While the locations of the ice around Antarctica are in agreement with observations (Gersonde et al., 2005), the model underestimates the ice extent over the Weddell Sea and between the Weddell and Ross Seas. The lack of ice is partly attributable to a warm bias in the Southern Ocean associated with the previously mentioned weak ACC (discussed further below). During August and September, simulated sea ice is greatly reduced in the North Atlantic region (Fig. 11), with remnant ice persisting in the extreme north of Baffin Bay and the east coast of Greenland, also in agreement with observations. In the SH, the corresponding winter sea ice grows substantially and the distribution is in generally good agreement with observations (Gersonde et al., 2005).

The simulated annual average ice extents for the NH are 9.8×10^6 km^2 for the LGM, 15.8×10^6 km^2 for 6 ka and 14.1×10^6 km^2 for PI (grid cells with fractional coverage > 15%). Compounded with climate-forcing, changes in both the distribution and areal coverage of the NH ice also reflect the change in ocean area due to the transition of land and ice sheets to ocean as sea level rises (Fig. 11 and SFigs. 13 - 15). For the same time

Jay Alder 12/28/14 9:24 AM
Comment: R2: It should be made clear in the beginning that NH sea ice area extent is controlled by bathymetry (land-sea-area changes). Area changes are in response to external forcing are thus biased.

Jay Alder 12/28/14 9:24 AM
Comment: R1: “simulated sea-ice fraction”. Firstly, the authors discuss sea ice area, not fraction.
Secondly, in fact sea ice area in the NH is increasing (not decreasing) from LGM to Holocene because of increasing Arctic ocean area.

Steve 1/16/15 8:31 AM
Deleted: Changes in both the distribution and areal coverage of the NH ice reflect the transition of land and ice sheets to ocean in the model surface-type maps as sea level risesIn both hemispheres, simulated sea-ice fractions display a decreasing trend from the LGM through the early Holocene in response to global warming and obliquity-related changes in insolation (Fig. 11 and SFigs. 13 - 15).

Jay Alder 12/15/14 3:02 PM
Deleted: .

Jay Alder 12/15/14 2:57 PM
Deleted: Changes in both the distribution and areal coverage of the NH ice reflect the transition of land and ice sheets to ocean in the model surface-type maps as sea level rises.

Steve 1/16/15 8:31 AM
Deleted: ,

Steve 1/16/15 8:34 AM
Deleted: reflecting the change in ocean area

periods, the SH ice area extents, which are minimally affected by land-sea transitions with sea level rise, are 20.9×10^6 km^2, 11.4×10^6 km^2 and 11.1×10^6 km^2, respectively.

During the 21 ka boreal winter, the Arctic Ocean and Baffin Bay are fully covered by ice and the ice around Greenland expands. The model displays increased sea ice in the western North Atlantic and decreased ice in the eastern North Atlantic and Nordic Seas where the prescribed FIS margin advances into the water (Fig. 2). The limit of substantial coverage north of 55°N is in agreement with reconstructions (de Vernal et al., 2006) and other LGM simulations (Otto-Bliesner et al., 2006a; Roche et al., 2007); however, slight fractional cover (pack ice) in the model likely extends too far south (to ~45°N) along the coast of North America. Fractional cover of up to 100% is simulated in the far Northwest Pacific and the Sea of Okhotsk with a sharp, southward transition to reduced coverage. In boreal summer of the LGM, simulated sea ice retreats to 65°N in the North Atlantic and persists along eastern Canada, Baffin Bay and south of Greenland and the extreme northern areas of the Nordic Seas.

The overall distribution of SH sea ice (Fig. 11) is in good agreement with reconstructions and other model simulations (Gersonde et al., 2005; Roche et al., 2012). The simulated LGM maximum winter sea ice area is 35.5 ×10^6 km^2 (72% greater than PI) and the LGM summer minimum is 4.8×10^6 km^2 (112% greater than PI); the winter and summer reconstructed areas are 43.5 ± 4 ×10^6 km^2 and 11.1 ± 4 ×10^6 km^2, respectively (Roche et al., 2012). The seasonal amplitude (maximum minus minimum) of LGM ice cover simulated by GENMOM (30.6 × 10^6 km^2) is comparable with the reconstructed amplitude (32.4 ± 4×10^6 km^2) and the LGM-to-PI change of seasonality is well within the range simulated by the PMIP2 models (Roche et al., 2012 their Figures 2 and 3).

Steve 1/16/15 8:35 AM
Comment: Not meaning at all or minimally?

Steve 1/16/15 8:34 AM
Deleted: area changes

Jay Alder 12/28/14 9:24 AM
Comment: R2: It would be better to write 'not affected by land-sea area changes with global sea level rise' (in this model at least; ice-shelf changes could indeed change the ocean area for sea ice)

Steve 1/16/15 8:35 AM
Deleted: global

Jay Alder 12/15/14 3:01 PM
Deleted: not affected by rising sea level

Jay Alder 12/15/14 3:11 PM
Deleted: captures the spatial distribution of

Jay Alder 12/15/14 3:13 PM
Deleted: more

Jay Alder 12/15/14 3:13 PM
Deleted: less

Jay Alder 12/28/14 9:24 AM
Comment: R1: "The model captures the spatial distribution of more sea ice…". Please reformulate

3.5 Antarctic Circumpolar Current and Atlantic Meridional Overturning Circulation

The simulated ACC of 62 Sv is ~48% weaker than the observed value of 119 Sv through the Drake Passage (GECCO data; Köhl and Stammer, 2008). Although the T31 resolution of GENMOM is a factor in limiting flow through the Drake Passage, we attribute the underestimate of the ACC in part to insufficient wind stress at the latitude of the Drake Passage, which is caused by equatorward displacement of the core of the westerly winds, a shortcoming in common with other low-resolution AOGCMs (Alder et al., 2011; Russell et al., 2006; Schmittner et al., 2011a).

Considerable uncertainty exists in the proxies that are used to infer past changes in AMOC strength (Delworth and Zeng, 2008; Lynch-Stieglitz et al., 2007). The $^{231}Pa/^{230}Th$ record from 33°N on the Bermuda Rise (Lippold et al., 2009; McManus et al., 2004) indicates that after the LGM the strength of the AMOC began to diminish at ~18 ka, was further reduced during Heinrich Event 1 (H1) at ~17 ka, increased abruptly during the BA at 15 ka, and weakened again during the YD cold reversal at ~12 ka. After the YD, the AMOC strengthened again and stabilized. In climate models, a variety of factors including the North Atlantic freshwater budget, model resolution and parameterizations and the characteristics of simulated Antarctic Bottom Water (AABW) give rise to a considerable simulated range of AMOC (Weber et al., 2007).

The AMOC in our PI simulation (Fig. 12) is 19.3 ± 1.4 Sv at the core site of 33°N, a value similar to the present-day estimate of 18.7 ± 4.8 Sv at 26.5°N (Srokosz et al., 2012). The maximum AMOC simulated by GENMOM in the PI is 21.3 Sv at 41°N, a value outside the range of 13.8 to 20.8 Sv of five models in the PMIP2 experiments (Weber et al., 2007), but within the range of 3.8 to 31.7 Sv of the IPCC AR4

Jay Alder 12/15/14 4:14 PM
Deleted: ~2 Sv greater than

Jay Alder 12/15/14 4:12 PM
Deleted: 17

Jay Alder 12/15/14 4:12 PM
Deleted: 4

Jay Alder 12/28/14 9:24 AM
Comment: R1: IPCC AR5 report is now available. Please cite it instead of AR4.

models (Schmittner et al., 2005). The newer CMIP5 models have a narrower range of AMOC of ~14 to ~30 Sv when sampled at 30°N {Cheng:2013ef}; GENMOM simulates 16.0 ± 1.3 Sv at this location.

Our simulated LGM AMOC at the core site is 16.4 Sv, which is a ~14.7% reduction relative to the PI. The maximum LGM AMOC is 22.4 Sv at 40.8°N, an increase of 1.1 Sv (5.1%) relative to the PI maximum and within the considerable range of -6.2 to +7.3 Sv in five PMIP2 simulations (Weber et al., 2007). In the deglacial simulations (21 ka through 15 ka), the northward (positive) AMOC flow extends deeper than that of the PI (Fig. 12) and the southward flow or AABW consequently is somewhat weakened. The maximum AMOC in GENMOM is essentially constant at 40.8°N depth of 1.23 km for all time slices. Although the depth of the maximum is again comparable to the range of the PMIP2 models (1.24 ± 0.20), the invariance of the location and depth in GENMOM is likely a model-specific response.

Our time slice simulations display an increase in the strength of AMOC from the LGM to a maximum at 15 ka, decrease to a minimum at 9 ka, and remain more-or-less constant through the PI (Fig. 13), which is in apparent disagreement with the $^{231}Pa/^{230}Th$ records from which greater variability is inferred (Lippold et al., 2009; McManus et al., 2004). We do not expect to capture rapid and abrupt climate change events such as H1 (~17 ka), the BA (~15 ka) and the YD (~12 ka) with only eight time slices, because we did not manipulate freshwater discharge to the North Atlantic in our experimental design.

4 21 ka and 6 ka data-model comparisons

We compare temperature and precipitation from our LGM and mid-Holocene simulations with paleoclimatic reconstructions and the PMIP3 simulations. For the LGM,

Jay Alder 12/15/14 4:01 PM
Deleted: Meehl et al., 2007;

Jay Alder 12/15/14 4:01 PM
Deleted: Analyses of AMOC in the IPCC AR5 and PMIP3 simulations are forthcoming.

Steve 1/16/15 8:37 AM
Deleted: , where

Jay Alder 12/28/14 9:24 AM
Comment: R2: Please take into consideration the recent study by Marson et al, Clim. Past, (2014) (doi:201410.5194/cp-10-1723-2014)

Jay Alder 12/8/14 1:48 PM
Deleted: segments

Jay Alder 12/17/14 9:45 AM
Deleted: ±

Jay Alder 12/8/14 1:48 PM
Deleted: -segment

Jay Alder 12/8/14 1:48 PM
Deleted: segments

we use the pollen-based reconstructions of mean annual mean temperature (MAT) and precipitation (MAP) from Bartlein et al. (2011) over land, and the Multiproxy Approach for the Reconstruction of the Glacial Ocean Surface Project (MARGO) reconstructions over oceans (Waelbroeck et al., 2009). The gridded 2° x 2° pollen data include >3,000 terrestrial pollen records from Eurasia, Africa and North America, and the global MARGO reconstruction comprises ~700 analyses of planktonic foraminifera, diatom, dinoflagellate cyst and radiolarian abundances, alkenones, and planktonic foraminifera Mg/Ca from marine core sites. For 6 ka, we combine the pollen-based reconstructions of Bartlein et al. (2011) and the GHOST SST reconstructions (Leduc et al., 2010). The 6 ka GHOST data set contains ~100 reconstructed temperature records based on analyses of alkenones and foraminifera Mg/Ca from marine sites located along continental margins and the Mediterranean Sea.

4.1 21 ka

Our simulated 21 ka anomalies of MAT and MAP are comparable with the pollen reconstructions (Fig. 14) and fall within the range of the PMIP3 models. GENMOM captures the mixed pattern of temperature and precipitation anomalies over Beringia that are present in the reconstructions (Fig. 14a,b) and in several of the PMIP3 simulations (SFigs. 8, 9, and 16). The GENMOM SST anomalies indicate broad cooling of the global oceans (mean of -1.7 °C) but not as much cooling as is simulated in the PMIP3 models (mean of -2.9 °C); although, Harrison et al. (2013) found that the PMIP3 models tended to overestimate oceanic cooling. Sampled at the MARGO locations, GENMOM is generally warmer, but within the range of the PMIP3 models {Harrison:2013jq}. The overall agreement of the simulation with the MARGO data is good, but some features in

Steve 1/16/15 9:17 AM
Deleted: When s

the MARGO data are not reproduced by GENMOM. For example, similar to the PMIP3 simulations (SFigs. 5, 6 and 16) the GENMOM simulation lacks the warming over the Greenland and Nordic Seas inferred from the data; although, while the data indicate the Nordic Sea was ice free at the LGM, the magnitude of the warming elsewhere, if it occurred, is somewhat unclear (de Vernal et al., 2006; Moller et al., 2011). The limited cooling along the western coast of North America and Mediterranean in GENMOM is attributed to the inability of the model to resolve the California Current and the Mediterranean circulation (Alder et al., 2011).

Over the tropical ocean basins, the 21 ka GENMOM simulation is 1.6 °C colder than the PI, in good agreement with the inferred MARGO cooling of 1.7 ± 1 °C (Otto-Bliesner et al., 2009). Average simulated SST anomalies are also similar to MARGO over the Indian (-1.6 °C versus -1.4 ± 0.7 °C) and Pacific (-1.5 °C versus -1.2 ± 1.1 °C) Oceans, but are warmer than the data in the tropical Atlantic basin (-1.9 °C versus -2.9 ± 1.3 °C). In each of these regions, the anomalies simulated by GENMOM fall within the range of six PMIP2 models analyzed by Otto-Bliesner et al. {*OttoBliesner:2009bw}. GENMOM captures the 2 – 4 °C cooling in the eastern coastal Atlantic evident in the MARGO data, and the SST anomalies are ~2 – 4 °C colder over the Western Pacific Warm Pool. Neither GENMOM nor the PMIP3 simulations produce the warming over the central and eastern tropics, or the low latitudes and the North Atlantic that is evident in the MARGO reconstruction.

The simulated LGM MAP anomalies are also comparable with the pollen-based reconstructions (Fig. 14c and d). The model simulates general drying of the NH and a mix of increased and decreased precipitation in Beringia, South America, southern

Jay Alder 12/17/14 9:45 AM
Deleted: ±

Jay Alder 12/17/14 9:44 AM
Deleted: ±

Jay Alder 12/17/14 9:44 AM
Deleted: ±

Jay Alder 12/17/14 9:44 AM
Deleted: ±

Steve 1/16/15 9:18 AM
Deleted: values

Africa, Southeast (SE) Asia and Australia. GENMOM produces strong drying over and around the NH ice sheets, wetter-than-present conditions in the southwestern United States and drying in Central America. The simulation fails to reproduce the drying over eastern North America that is inferred from the pollen-based data. There is considerable variability in the PMIP3 simulations of MAP (SFigs. 9 and 10). In common with the PMIP3 models, GENMOM simulates a general reduction of precipitation over the NH, the North African and Indian monsoon regions, and SE Asia, and increased precipitation south of the LIS, southern Africa and much of Australia (SFig. 16).

4.2 6 ka

Relative to PI, the changes in 6 ka boundary conditions are predominantly in the seasonality of insolation (Table 1) as opposed to the stronger radiative forcing associated with changes in GHGs and continental ice sheets from the LGM through the early Holocene. The resulting changes in 6 ka climatology are thus more subtle than those of the deglaciation. The changes of 6 ka MAT simulated by GENMOM are generally within the range of ±1 °C (Fig. 15b). Enhanced MAP and associated cooling are evident in the NH monsoonal regions (Fig. 15d). Elsewhere, MAP changes are within a range of ±50 mm.

Pollen-based data reconstructions indicate highly heterogeneous changes in MAT during 6 ka; however, there are regions with spatially consistent changes in sign, such as warming south of Hudson Bay, areas of warming over Scandinavia and Western Europe, and cooling in the Mediterranean region (Fig. 15a). Larger MAT changes at high-elevation sites and regions with anomalies of mixed sign occur in the data over most continents. The GENMOM 6 ka MAT anomalies also display a mix of warming and

Jay Alder 12/28/14 9:24 AM
Comment: R2: I am confused by the use of the word ‘regionally coherent pattern’ and ‘contrasting areas of warming’. Is a coherent pattern a pattern with only positive (or negative) anomalies, whereas ‘contrasting areas’ show both positive and negative anomalies? Could it be labeled as ‘regionally incoherent pattern’? Or does the use of words suggest an inconsistency with a reference pattern (e.g. the pattern reconstructed by proxies)?

Steve 1/16/15 9:18 AM
Deleted: . H

Jay Alder 12/17/14 10:42 AM
Deleted: Regionally coherent patterns of temperature anomalies

Jay Alder 12/17/14 10:44 AM
Deleted: the

Jay Alder 12/17/14 10:42 AM
Deleted: the contrasting

Jay Alder 12/17/14 10:42 AM
Deleted: , are inferred by the pollen-based data

cooling in a range of about ±4 °C; however, where pollen-based records exist, the majority of the anomalies are within a narrower range of about ±1.5 °C (Fig. 15b). GENMOM, and many of the PMIP3 models (SFigs. 8, 9 and 16), produce a mixture of warm and cold 6 ka MAT anomalies that are generally in the range of ±1 °C over the North Atlantic, Europe and Scandinavia, which underestimates the proxy-based anomalies by >2 °C at some sites.

The Asian pollen-based reconstruction similarly displays a heterogeneous temperature pattern that is reproduced by GENMOM and the PMIP3 models. In all of the models, the sign of the anomalies does not vary abruptly in close proximity to the pollen sites. We note, however, that the smooth topography in GCMs limits the ability of the models to reproduce large and regionally spatially heterogeneous anomalies that are characteristic of the local climate at many high elevation pollen sites in Western North America, the Alps, the central plateau of African and Asia.

GENMOM displays cooling in the North African and Indian monsoon regions and warming over the high northern latitudes, consistent with the PMIP3 models (Fig. 15). In contrast, GENMOM simulates weak global cooling of 0.39 °C compared to no change in the PMIP3 model average which is partially attributed to our lower prescribed GHG concentrations (Table 1 caption).

Precipitation anomalies inferred from the pollen-based data indicate that 6 ka was wetter than the PI in Europe, Africa, Asia and some parts of western North America and drier than PI in much of eastern North America and Scandinavia (Fig. 15c). GENMOM simulates the gradients and coherent patterns of positive and negative MAP anomalies over North America, and North, Central and western Africa, in agreement with the data and the PMIP3 models. The data and GENMOM are also in agreement over the Asian monsoon region and northwest Asia where wetter conditions prevail, but anomalies of opposite sign are simulated over the Great Lowland Plain in north central Eurasia and Southeast Asia. Bartlein et al. (2011) attribute cooling in Southeast Asia to a stronger winter monsoon at 6 ka. Our results (Figs. 6a and 8a), and many of the PMIP3 models, indicate cooler, drier winters (SFigs. 7 and 11) and regionally variable changes in the summer (SFigs. 8 and 12).

In Africa, the model captures the increase in precipitation in the northern and continental regions and drying along the southern coastal regions, as evident in the data. Strengthening of the African and Indian summer monsoons during the mid-Holocene corresponds well with the PMIP2 and PMIP3 models (Zheng and Braconnot, 2013). Both GENMOM and the data indicate drying over central Scandinavia, wetter conditions over east central Europe, the Iberian Peninsula and around the Mediterranean but, over Western Europe, the simulated decrease in MAP in GENMOM clearly disagrees with the data and some of the PMIP3 models (Figs. 15, SFigs. 7, 8 and 16); although, the magnitude of the change in the models is very small and the sign of the change varies among models. Wetter conditions also prevail in Indonesia, and a southwest-to-northeast wet-dry gradient is simulated over Australia.

5 Summary

We have presented a suite of multi-century equilibrium climate simulations with GENMOM for the past 21,000 years at 3,000-yr intervals. Each 1,100-yr simulation was forced with fixed, time-appropriate global boundary conditions that included insolation, GHGs, continental ice sheets and adjustment for sea level. The key drivers of climate change from the LGM through the Holocene are retreat of the NH ice sheets, deglacial increased of GHG concentrations, and latitudinal and seasonal variations in insolation.

GENMOM reproduces reasonably well the LGM to Holocene temperature trends inferred from the paleoclimate data syntheses of Shakun et al. (2012) and Marcott et al. (2013). The evolution of global temperature change simulated by GENMOM is consistent with three transient simulations, but is generally cooler during the deglacial time slices than the transient simulations when sampled at the proxy locations. The global LGM cooling of 3.8 °C simulated by GENMOM is within the range of 2.6 to 5.0 °C and average of 4.4 °C simulated by the PMIP3 models. Simulated LGM cooling of the tropical oceans is 1.6 °C, which is in good agreement with the MARGO reconstruction of 1.7 ± 1 °C. The weaker LGM global cooling is attributed to the sensitivity of GENMOM to CO_2 (2.2 °C for a 2X increase in the present-day value).

During the LGM, simulated precipitation is reduced globally by 8.2% and gradually increases through the Holocene to present-day values in response to loss of the NH ice sheets, global warming and related increases in atmospheric humidity. Between 15 ka and 6 ka seasonal changes in insolation altered the NH land-sea temperature contrasts, which, combined with shifts in global circulation, strengthened the summer monsoons in Africa and India. Monsoonal precipitation in both regions peaked between 12 ka and 9 ka, consistent with pollen-based reconstructions. The spatial patterns of mid-Holocene precipitation change simulated by GENMOM correspond well with the PMIP3 models, as do the 6 ka changes in monsoonal precipitation. In contrast to the pollen-based reconstructions, GENMOM simulates slightly drier instead of slightly wetter-than-present in Western Europe.

Steve 1/16/15 9:19 AM
Deleted: GENMOM simulated

Jay Alder 12/17/14 11:03 AM
Deleted: 2.6 to 4.9

Jay Alder 12/17/14 9:44 AM
Deleted: ±

Jay Alder 12/17/14 12:27 PM
Deleted: The

Steve 1/16/15 9:20 AM
Deleted: Relative to other PMIP models, t

Jay Alder 12/17/14 12:29 PM
Deleted: magnitude of the global LGM

Jay Alder 12/28/14 9:24 AM
Comment: R2: Climate sensitivity was found to be on the low end for doubling CO2. If the LGM cooling is now consistent and in the middle range of the estimated LGM cooling, I wonder would that indicate a higher climate sensitivity during the LGM (a result suggesting a 'state-dependent' climate sensitivity?) or is it suggesting that the cooling contribution from ice-sheets (here an external forcing) is overestimated / or proxies may underestimate the global cooling contribution (e.g. they may not sample appropriately the NH ice-sheet regions). Or is the climate sensitivity and LGM cooling altogether consistent within the margin of uncertainties?

The eight time slice simulations depict the glacial-interglacial transition that is in good agreement with other AOGCM simulations and compares reasonably well with data-based climate reconstructions. The simulations provide insights into key dynamic features of the transition, such as altered NH storm tracks and strengthening of monsoons during the early to mid-Holocene. The data-model and model-model comparisons give us a measure of confidence that our paleo GENMOM simulations are reasonable on broad spatial scales and adds to the growing number of climate models that are capable of simulating key aspects of past climate change when constrained by a relatively small set of global boundary conditions. Future work using the model output produced by this study will address how internal model variability and multidecadal variability influence comparison with proxy data, particularly in North America using dynamical downscaling techniques.

Jay Alder 12/17/14 10:49 AM
Formatted: Body

Jay Alder 12/8/14 1:48 PM
Deleted: segment

Jay Alder 12/17/14 10:49 AM
Deleted:

Appendix A: List of abbreviations and acronyms

AABW	Antarctic Bottom Water
ACC	Antarctic Circumpolar Current
AMOC	Atlantic Meridional Overturning Circulation
AOGCM	Atmosphere-Ocean General Circulation Model
BA	Bølling-Allerød
CIS	Cordilleran Ice Sheet
CLIMAP	Climate: Long range Investigation, Mapping, and Prediction
COHMAP	Cooperative Holocene Mapping Project
DJF	December, January and February
FIS	Fennoscandian Ice Sheet
GECCO	German partner of Estimating the Circulation and Climate of the Ocean
GENESIS	Global Environmental and Ecological Simulation of Interactive Systems
GHG	Greenhouse gas
ITCZ	Intertropical Convergence Zone
H1	Heinrich Event 1
JJA	June, July and August
LGM	Last Glacial Maximum
LIS	Laurentide Ice Sheet
LSX	Land Surface eXchange
MAM	March, April and May
MAP	Mean annual precipitation
MARGO	Multiproxy Approach for the Reconstruction of the Glacial Ocean Surface Project
MAT	Mean annual temperature
MOM2	Modular Ocean Model version 2
NCAR	National Center for Atmospheric Research
NCEP	National Centers for Environmental Prediction
NH	Northern Hemisphere
OSU-LIS	Oregon State University Laurentide Ice Sheet
PD	Present-day
PI	Pre-industrial
PMIP	Palaeoclimate Modelling Intercomparison Project
SH	Southern Hemisphere
SLP	Sea-level pressure
SON	September, October and November
SST	Sea surface temperature
TEMPO	Testing Earth System Models with Paleoenvironmental Observations
YD	Youger Dryas

Acknowledgments

We thank P. Bartlein, J. Shakun, S. Marcott, the MARGO and GHOST project members for providing their proxy reconstructions. Z. Liu and J. Zhu kindly provided time series data for the three transient models CCSM3, LOVECLIM and FAMOUS. We thank P. Bartlein, D. Pollard and R. Thompson for their thoughtful reviews and A. Schmittner, S. Marcott and P. Clark for helpful discussions and insights.

References

Alder, J. R., Hostetler, S. W., Pollard, D. and Schmittner, A.: Evaluation of a present-day climate simulation with a new coupled atmosphere-ocean model GENMOM, Geosci. Model Dev., 4(1), 69–83, doi:10.5194/gmd-4-69-2011, 2011.

Annan, J. D. and Hargreaves, J. C.: A new global reconstruction of temperature changes at the Last Glacial Maximum, Clim Past, 9(1), 367–376, doi:10.5194/cp-9-367-2013, 2013.

Bartlein, P. J., Harrison, S. P., Brewer, S., Connor, S., Davis, B. A. S., Gajewski, K., Guiot, J., Harrison-Prentice, T. I., Henderson, A., Peyron, O., Prentice, I. C., Scholze, M., Seppä, H., Shuman, B., Sugita, S., Thompson, R. S., Viau, A. E., Williams, J. and Wu, H.: Pollen-based continental climate reconstructions at 6 and 21 ka: a global synthesis, Clim Dynam, 37(3-4), 775–802, doi:10.1007/s00382-010-0904-1, 2011.

Beckmann, B., Flogel, S., Hofmann, P., Schulz, M. and Wagner, T.: Orbital forcing of Cretaceous river discharge in tropical Africa and ocean response, Nature, 437(7056), 241–244, doi:10.1038/nature03976, 2005.

Berger, A. and Loutre, M. F.: Insolation values for the climate of the last 10 million years, Quaternary Sci Rev, 1991.

Bice, K. L., Birgel, D., Meyers, P. A., Dahl, K. A., Hinrichs, K. U. and Norris, R. D.: A multiple proxy and model study of Cretaceous upper ocean temperatures and atmospheric CO2 concentrations, Paleoceanography, 21(2), doi:10.1029/2005PA001203, 2006.

Braconnot, P., Harrison, S. P., Kageyama, M., Bartlein, P. J., Masson-Delmotte, V., Abe-Ouchi, A., Otto-Bliesner, B. L. and Zhao, Y.: Evaluation of climate models using palaeoclimatic data, Nat Geosci, 2(6), 417–424, doi:10.1038/nclimate1456, 2012.

Braconnot, P., Otto-Bliesner, B. L., Harrison, S., Joussaume, S., Peterschmitt, J. Y., Abe-Ouchi, A., Crucifix, M., Driesschaert, E., Fichefet, T., Hewitt, C. D., Kageyama, M., Kitoh, A., Laîné, A., Loutre, M. F., Marti, O., Merkel, U., Ramstein, G., Valdes, P., Weber, S. L., Yu, Y. and Zhao, Y.: Results of PMIP2 coupled simulations of the Mid-Holocene and Last Glacial Maximum - Part 1: experiments and large-scale features, Clim Past, 3(2), 261–277, 2007a.

Braconnot, P., Otto-Bliesner, B. L., Harrison, S., Joussaume, S., Peterschmitt, J. Y., Abe-Ouchi, A., Crucifix, M., Driesschaert, E., Fichefet, T., Hewitt, C. D., Kageyama, M., Kitoh, A., Loutre, M. F., Marti, O., Merkel, U., Ramstein, G., Valdes, P., Weber, L., Yu, Y. and Zhao, Y.: Results of PMIP2 coupled simulations of the Mid-Holocene and Last Glacial Maximum - Part 2: feedbacks with emphasis on the location of the ITCZ and mid- and high latitudes heat budget, Clim Past, 3(2), 279–296, 2007b.

Broccoli, A. J., Dahl, K. A. and Stouffer, R. J.: Response of the ITCZ to Northern

Hemisphere cooling, Geophys. Res. Lett., 33(1), doi:10.1029/2005GL024546, 2006.

Brohan, P., Kennedy, J. J., Harris, I., Tett, S. F. B. and Jones, P. D.: Uncertainty estimates in regional and global observed temperature changes: A new data set from 1850, J.-Geophys.-Res., 111(D12), doi:10.1029/2005JD006548, 2006.

Brook, E. J., Harder, S., Severinghaus, J., Steig, E. J. and Sucher, C. M.: On the origin and timing of rapid changes in atmospheric methane during the last glacial period, Global Biogeochem Cy, 14(2), 559–572, 2000.

Cheng, H., Sinha, A., Wang, X., Cruz, F. W. and Edwards, R. L.: The Global Paleomonsoon as seen through speleothem records from Asia and the Americas, Clim Dynam, 39(5), 1045–1062, doi:10.1007/s00382-012-1363-7, 2012.

Chiang, J. C. H.: The Tropics in Paleoclimate, Annual Review of Earth and Planetary Sciences, 37, 263–297, doi:10.1146/annurev.earth.031208.100217, 2009.

Chiang, J. C. H. and Bitz, C. M.: Influence of high latitude ice cover on the marine Intertropical Convergence Zone, Clim Dynam, 25(5), 477–496, doi:10.1007/s00382-005-0040-5, 2005.

Clark, P. U., Shakun, J. D., Baker, P. A., Bartlein, P. J., Brewer, S., Brook, E., Carlson, A. E., Cheng, H., Kaufman, D. S., Liu, Z. Y., Marchitto, T. M., Mix, A. C., Morrill, C., Otto-Bliesner, B. L., Pahnke, K., Russell, J. M., Whitlock, C., Adkins, J. F., Blois, J. L., Clark, J., Colman, S. M., Curry, W. B., Flower, B. P., He, F., Johnson, T. C., Lynch-Stieglitz, J., Markgraf, V., McManus, J., Mitrovica, J. X., Moreno, P. I. and Williams, J. W.: Global climate evolution during the last deglaciation, P Natl Acad Sci USA, 109(19), E1134–E1142, doi:10.1073/Pnas.1116619109, 2012.

CLIMAP Project Members: Seasonal reconstructions of the earth's surface at the Last Glacial Maximum, Geological Society of America, 18, 1981.

COHMAP Members: Climatic Changes of the Last 18,000 Years - Observations and Model Simulations, Science, 241(4869), 1043–1052, 1988.

de Vernal, A., Rosell-Mele, A., Kucera, M., Hillaire-Marcel, C., Eynaud, F., Weinelt, M., Dokken, T. and Kageyama, M.: Comparing proxies for the reconstruction of LGM sea-surface conditions in the northern North Atlantic, Quaternary Sci Rev, 25(21-22), 2820–2834, doi:10.1016/j.quascirev.2006.06.006, 2006.

DeConto, R. M., Pollard, D. and Harwood, D.: Sea ice feedback and Cenozoic evolution of Antarctic climate and ice sheets, Paleoceanography, 22(3), doi:10.1029/2006PA001350, 2007.

DeConto, R. M., Pollard, D., Wilson, P. A., Palike, H., Lear, C. H. and Pagani, M.: Thresholds for Cenozoic bipolar glaciation, Nature Geoscience, 455(7213), 652–U52, doi:10.1038/nature07337, 2008.

Delworth, T. L. and Zeng, F.: Simulated impact of altered Southern Hemisphere winds on the Atlantic Meridional Overturning Circulation, Geophys. Res. Lett., 35(20), doi:10.1029/2008gl035166, 2008.

DiNezio, P. N. and Tierney, J. E.: The effect of sea level on glacial Indo-Pacific climate, Nature Geoscience, 6(6), 1–7, doi:10.1038/ngeo1823, 2013.

Dorman, J. L. and Sellers, P. J.: A Global Climatology of Albedo, Roughness Length and Stomatal-Resistance for Atmospheric General-Circulation Models as Represented by the Simple Biosphere Model (Sib), J Appl Meteorol, 28(9), 833–855, doi:10.1175/1520-0450(1989)028<0833:Agcoar>2.0.Co;2, 1989.

Dyke, A. S. and Prest, V. K.: Late Wisconsinan and Holocene history of the Laurentide ice sheet, Géographie physique et Quaternaire, 1987.

Felzer, B.: Climate impacts of an ice sheet in East Siberia during the Last Glacial Maximum, Quaternary Sci Rev, 20(1-3), 437–447, doi:10.1016/S0277-3791(00)00106-2, 2001.

Felzer, B., Oglesby, R. J., Webb, T. and Hyman, D. E.: Sensitivity of a general circulation model to changes in northern hemisphere ice sheets, J.-Geophys.-Res., 101(D14), 19077–19092, 1996.

Felzer, B., Webb, T. and Oglesby, R. J.: The impact of ice sheets, CO2, and orbital insolation on late quaternary climates: Sensitivity experiments with a general circulation model, Quaternary Sci Rev, 17(6-7), 507–534, doi:10.1016/S0277-3791(98)00010-9, 1998.

Flato, G. M. and Hibler, W. D.: Modeling Pack Ice as a Cavitating Fluid, Journal of Physical Oceanography, 22(6), 626–651, 1992.

Gasse, F.: Hydrological changes in the African tropics since the Last Glacial Maximum, Quaternary Sci Rev, 19(1-5), 189–211, doi:10.1016/S0277-3791(99)00061-X, 2000.

Gates, W. L. and Nelson, A. B.: A new (revised) tabulation of the Scripps topography on a 1 degree global grid. Part 1: Terrain heights, Tech. Rep. R-1276-1-ARPA. 1975.

Gent, P. R. and McWilliams, J. C.: Isopycnal mixing in ocean circulation models, Journal of Physical Oceanography, 1990.

Gersonde, R., Crosta, X., Abelmann, A. and Armand, L.: Sea-surface temperature and sea ice distribution of the Southern Ocean at the EPILOG Last Glacial Maximum—a circum-Antarctic view based on siliceous microfossil records, Quaternary Sci Rev, 24(7-9), 869–896, doi:10.1016/j.quascirev.2004.07.015, 2005.

Harrison, S.: Harrison et al SI Clim Dynam 2013,, 1–42, 2013.

Harrison, S. P., Bartlein, P. J., Brewer, S., Prentice, I. C., Boyd, M., Hessler, I., Holmgren, K., Izumi, K. and Willis, K.: Climate model benchmarking with glacial and mid-Holocene climates, Clim Dynam, doi:10.1007/s00382-013-1922-6, 2013.

Harvey, L. D. D.: Development of a Sea Ice Model for Use in Zonally Averaged Energy Balance Climate Models, J Climate, 1(12), 1221–1238, 1988.

Hassol, S. J.: Impacts of a Warming Arctic - Arctic Climate Impact Assessment, Impacts of a Warming Arctic - Arctic Climate Impact Assessment, by Arctic Climate Impact Assessment, pp. 144. ISBN 0521617782. Cambridge, UK: Cambridge University Press, December 2004., -1, 2004.

Hély, C., Braconnot, P., Watrin, J. and Zheng, W.: Climate and vegetation: Simulating the African humid period, Comptes Rendus Geoscience, 341(8-9), 671–688, doi:10.1016/j.crte.2009.07.002, 2009.

Horton, D. E., Poulsen, C. J. and Pollard, D.: Orbital and CO2 forcing of late Paleozoic continental ice sheets, Geophys. Res. Lett., 34(19), doi:10.1029/2007GL031188, 2007.

Hostetler, S. W., Clark, P. U., Bartlein, P. J., Mix, A. C. and Pisias, N. J.: Atmospheric transmission of North Atlantic Heinrich events, J.-Geophys.-Res., 104(D4), 3947–3952, 1999.

Hostetler, S. W., Pisias, N. and Mix, A. C.: Sensitivity of Last Glacial Maximum climate to uncertainties in tropical and subtropical ocean temperatures, Quaternary Sci Rev, 25(11-12), 1168–1185, doi:10.1016/j.quascirev.2005.12.010, 2006.

Jaccard, S. L., Haug, G. H., Sigman, D. M., Pedersen, T. F., Thierstein, H. R. and Rohl, U.: Glacial/interglacial changes in subarctic North Pacific stratification, Science, 308(5724), 1003–1006, doi:10.1126/science.1108696, 2005.

Joussaume, S., Taylor, K. E., Braconnot, P., mitchell, J., Kutzbach, J. E., Harrison, S. P., Prentice, I. C., Broccoli, A. J., Abe-Ouchi, A., Bartlein, P. J., Bonfils, C., Dong, B., Guiot, J., Herterich, K., Hewitt, C. D., Jolly, D., Kim, J. W., Kislov, A., Kitoh, A., Loutre, M. F., Masson, V., McAvaney, B., McFarlane, N., de Noblet, N., Peltier, W. R., Peterschmitt, J. Y., Pollard, D., Rind, D., Royer, J. F., Schlesinger, M. E., Syktus, J., Thompson, S. L., Valdes, P., Vettoretti, G., Webb, R. S. and Wyputta, U.: Monsoon changes for 6000 years ago: Results of 18 simulations from the Paleoclimate Modeling Intercomparison Project (PMIP), Geophys. Res. Lett., 26(7), 859–862, 1999.

Kageyama, M., D'Andrea, F., Ramstein, G., Valdes, P. J. and Vautard, R.: Weather regimes in past climate atmospheric general circulation model simulations, Clim Dynam, 15(10), 773–793, doi:10.1007/S003820050315, 1999.

Kageyama, M., Laîné, A., Abe-Ouchi, A., Braconnot, P., Cortijo, E., Crucifix, M., de Vernal, A., Guiot, J., Hewitt, C. D. and Kitoh, A.: Last Glacial Maximum temperatures over the North Atlantic, Europe and western Siberia: a comparison between PMIP models, MARGO sea–surface temperatures and pollen-based reconstructions, Quaternary Sci Rev, 25(17-18), 2082–2102, doi:10.1016/j.quascirev.2006.02.010, 2006.

Kalnay, E., Kanamitsu, M., Kistler, R., Collins, W., Deaven, D., Gandin, L., Iredell, M., Saha, S., White, G., Woollen, J., Zhu, Y., Chelliah, M., Ebisuzaki, W., Higgins, W., Janowiak, J., Mo, K. C., Ropelewski, C., Wang, J., Leetmaa, A., Reynolds, R., Jenne, R. and Joseph, D.: The NCEP/NCAR 40-year reanalysis project, Bull. Amer. Meteor. Soc., 77(3), 437–471, 1996.

Kiehl, J. T., Hack, J. J., Bonan, G. B., Boville, B. A., Williamson, D. L. and Rasch, P. J.: The National Center for Atmospheric Research Community Climate Model: CCM3, J Climate, 11(6), 1131–1149, 1998.

Kim, S.-J., Crowley, T. J., Erickson, D. J., Govindasamy, B., Duffy, P. B. and Lee, B. Y.: High-resolution climate simulation of the last glacial maximum, Clim Dynam, 31(1), 1–16, doi:10.1007/s00382-007-0332-z, 2007.

Köhl, A. and Stammer, D.: Decadal sea level changes in the 50-year GECCO ocean synthesis, J Climate, 21(9), 1876–1890, doi:10.1175/2007JCLI2081.1, 2008.

Kump, L. R. and Pollard, D.: Amplification of cretaceous warmth by biological cloud feedbacks, Science, 320(5873), 195–195, doi:10.1126/science.1153883, 2008.

Kutzbach, J. E. and Liu, Z.: Response of the African Monsoon to Orbital Forcing and Ocean Feedbacks in the Middle Holocene, Science, 278(5337), 440–443, doi:10.1126/science.278.5337.440, 1997.

Kutzbach, J. E. and Otto-Bliesner, B. L.: The Sensitivity of the African-Asian Monsoonal Climate to Orbital Parameter Changes for 9000 Years Bp in a Low-Resolution General-Circulation Model, Journal of the Atmospheric Sciences, 39(6), 1177–1188, 1982.

Kutzbach, J. E., Bartlein, P. J., FOLEY, J. A., Harrison, S. P., Hostetler, S. W., Liu, Z., Prentice, I. C. and WEBB, T. I.: Potential role of vegetation feedback in the climate sensitivity of high-latitude regions : A case study at 6000 years B.P, Global Biogeochem Cy, 10(4), 727–736, 1996a.

Kutzbach, J., Bonan, G., Foley, J. and Harrison, S. P.: Vegetation and soil feedbacks on the response of the African monsoon to orbital forcing in the early to middle Holocene, Nature, 384(6610), 623–626, doi:10.1038/384623a0, 1996b.

Kutzbach, J., Gallimore, R., Harrison, S., Behling, P., Selin, R. and Laarif, F.: Climate and biome simulations for the past 21,000 years, Quaternary Sci Rev, 17(6-7), 473–506, 1998.

Leduc, G., Schneider, R., Kim, J. H. and Lohmann, G.: Holocene and Eemian sea surface temperature trends as revealed by alkenone and Mg/Ca paleothermometry, Quaternary Sci Rev, 29(7-8), 989–1004, doi:10.1016/j.quascirev.2010.01.004, 2010.

Lee, J.-Y. and Wang, B.: Future change of global monsoon in the CMIP5, Clim Dynam, doi:10.1007/s00382-012-1564-0, 2012.

Li, C. and Battisti, D. S.: Reduced Atlantic Storminess during Last Glacial Maximum: Evidence from a Coupled Climate Model, J Climate, 21(14), 3561–3579, doi:10.1175/2007jcli2166.1, 2008.

Licciardi, J. M., Clark, P. U., Jenson, J. W. and Macayeal, D. R.: Deglaciation of a soft-bedded Laurentide Ice Sheet, Quaternary Sci Rev, 17(4-5), 427–448, doi:10.1016/S0277-3791(97)00044-9, 1998.

Lippold, J., Grützner, J., Winter, D., Lahaye, Y., Mangini, A. and Christl, M.: Does sedimentary231Pa/230Th from the Bermuda Rise monitor past Atlantic Meridional Overturning Circulation? Geophys. Res. Lett., 36(12), doi:10.1029/2009gl038068, 2009.

Liu, Z., Otto-Bliesner, B. L., He, F., Brady, E. C., Tomas, R., Clark, P. U., Carlson, A. E., Lynch-Stieglitz, J., Curry, W., Brook, E., Erickson, D., Jacob, R., Kutzbach, J. and Cheng, J.: Transient Simulation of Last Deglaciation with a New Mechanism for Bolling-Allerod Warming, Science, 325(5938), 310–314, doi:10.1126/science.1171041, 2009.

Lynch-Stieglitz, J., Adkins, J. F., Curry, W. B., Dokken, T., Hall, I. R., Herguera, J. C., Hirschi, J. J., Ivanova, E. V., Kissel, C., Marchal, O., Marchitto, T. M., McCave, I. N., McManus, J. F., Mulitza, S., Ninnemann, U., Peeters, F., Yu, E. F. and Zahn, R.: Atlantic meridional overturning circulation during the Last Glacial Maximum, Science, 316(5821), 66–69, doi:10.1126/science.1137127, 2007.

Marcott, S. A., Shakun, J. D., Clark, P. U. and Mix, A. C.: A Reconstruction of Regional and Global Temperature for the Past 11,300 Years, Science, 339(6124), 1198–1201, doi:10.1126/Science.1228026, 2013.

Marzin, C. and Braconnot, P.: Variations of Indian and African monsoons induced by insolation changes at 6 and 9.5 kyr BP, Clim Dynam, 33(2-3), 215–231, doi:10.1007/s00382-009-0538-3, 2009.

McManus, J. F., Francois, R., Gherardi, J. M., Keigwin, L. D. and Brown-Leger, S.: Collapse and rapid resumption of Atlantic meridional circulation linked to deglacial climate changes, Nature, 428(6985), 834–837, doi:10.1038/Nature02494, 2004.

Meehl, G. A., Stocker, T. F. and Collins, W. D.: Global climate projections, in Climate Change 2007: The Physical Science Basis. Contribution of Working Group I to the Fourth Assessment Report of the Intergovernmental Panel on Climate Change, edited by S. Solomon, D. Qin, M. Manning, Z. Chen, M. Marquis, K. B. Averyt, M. Tignor, and H. L. Miller, Cambridge University Press, Cambridge, United Kingdom and New York, NY, USA. 2007.

Miller, G., Mangan, J., Pollard, D., Thompson, S. L., Felzer, B. and Magee, J.: Sensitivity of the Australian Monsoon to insolation and vegetation: Implications for human impact on continental moisture balance, Geology, 33(1), 65–68, 2005.

Moller, T., Schulz, H. and Kucera, M.: The effect of sea surface properties on shell morphology and size of the planktonic foraminifer Neogloboquadrina pachyderma in the North Atlantic, Palaeogeography, 2011.

Monnin, E., Indermuhle, A., Dallenbach, A., Fluckiger, J., Stauffer, B., Stocker, T. F., Raynaud, D. and Barnola, J. M.: Atmospheric CO2 concentrations over the last glacial termination, Science, 291(5501), 112–114, 2001.

Otto-Bliesner, B. L., Brady, E. C., Clauzet, G., Tomas, R., Levis, S. and Kothavala, Z.: Last Glacial Maximum and Holocene climate in CCSM3, J Climate, 19(11), 2526–2544, doi:10.1175/Jcli3748.1, 2006a.

Otto-Bliesner, B. L., Schneider, R., Brady, E. C., Kucera, M., Abe-Ouchi, A., Bard, E., Braconnot, P., Crucifix, M., Hewitt, C. D., Kageyama, M., Marti, O., Paul, A., Rosell-Mele, A., Waelbroeck, C., Weber, S. L., Weinelt, M. and Yu, Y.: A comparison of PMIP2 model simulations and the MARGO proxy reconstruction for tropical sea surface temperatures at last glacial maximum, Clim Dynam, 32(6), 799–815, doi:10.1007/s00382-008-0509-0, 2009.

Otto-Bliesner, B. L., Tomas, R., Brady, E. C., Ammann, C., Kothavala, Z. and Clauzet, G.: Climate sensitivity of moderate- and low-resolution versions of CCSM3 to preindustrial forcings, J Climate, 19(11), 2567–2583, doi:10.1175/Jcli3754.1, 2006b.

Pacanowski, R. C.: MOM 2 Version 2.0 (Beta) Documentation: User's Guide and Reference Manual, NOAA GFDL Ocean Technical Report 3.2. 1996.

Pausata, F. S. R., Li, C., Wettstein, J. J., Kageyama, M. and Nisancioglu, K. H.: The key role of topography in altering North Atlantic atmospheric circulation during the last glacial period, Clim Past, 7(4), 1089–1101, doi:10.5194/cp-7-1089-2011, 2011.

Peixoto, J. P. and Oort, A. H.: Physics of Climate, Amer Inst of Physics. [online] Available from: http://adsabs.harvard.edu/cgi-bin/nph-data_query?bibcode=1992phcl.book.....P&link_type=CITATIONS, 1992.

Peltier, W. R.: Global glacial isostatic adjustment: palaeogeodetic and space-geodetic tests of the ICE-4G (VM2) model, Journal of Quaternary Science, 17(5-6), 491–510, doi:10.1002/jqs.713, 2002.

Pinot, S., Ramstein, G., Harrison, S. P., Prentice, I. C., Guiot, J., Stute, M. and Joussaume, S.: Tropical paleoclimates at the Last Glacial Maximum: comparison of Paleoclimate Modeling Intercomparison Project (PMIP) simulations and paleodata, Clim Dynam, 15(11), 857–874, 1999.

Pollard, D. and Reusch, D. B.: A calendar conversion method for monthly mean paleoclimate model output with orbital forcing, J.-Geophys.-Res., 107(D22), 4615, doi:10.1029/2002JD002126, 2002.

Pollard, D. and Thompson, S. L.: Sea-ice dynamics and CO2 sensitivity in a global climate model, Atmosphere-Ocean, 1994.

Pollard, D. and Thompson, S. L.: Use of a Land-Surface-Transfer Scheme (Lsx) in a Global Climate Model - the Response to Doubling Stomatal-Resistance, Global Planet Change, 10(1-4), 129–161, doi:10.1016/0921-8181(94)00023-7, 1995.

Pollard, D. and Thompson, S. L.: Climate and ice-sheet mass balance at the last glacial maximum from the genesis version 2 global climate model, Quaternary Sci Rev, 16(8), 841–863, 1997.

Pollard, D., Bergengren, J. C., Stillwell-Soller, L. M., Felzer, B. and Thompson, S. L.: Climate simulations for 10000 and 6000 years BP using the GENESIS global climate model. Palaeoclimates: Data and Modelling, Palaeoclimates - Data and Modelling. 1998.

Poulsen, C. J., Pollard, D. and White, T. S.: General circulation model simulation of the delta O-18 content of continental precipitation in the middle Cretaceous: A model-proxy comparison, Geology, 35(3), 199–202, doi:10.1130/G23343A.1, 2007a.

Poulsen, C. J., Pollard, D., Montanez, I. P. and Rowley, D.: Late Paleozoic tropical climate response to Gondwanan deglaciation, Geology, 35(9), 771–774, doi:10.1130/G23841A.1, 2007b.

Ramstein, G. and Joussaume, S.: Sensitivity experiments to sea surface temperatures, sea-ice extent and ice-sheet reconstruction for the Last Glacial Maximum, Annals of Glaciology, 1995.

Rind, D.: Components of the Ice-Age Circulation, J.-Geophys.-Res., 92(D4), 4241–4281, 1987.

Roche, D. M., Crosta, X. and Renssen, H.: Evaluating Southern Ocean sea-ice for the Last Glacial Maximum and pre-industrial climates: PMIP-2 models and data evidence, Quaternary Sci Rev, 56, 99–106, doi:10.1016/j.quascirev.2012.09.020, 2012.

Roche, D. M., Dokken, T. M., Goosse, H., Renssen, H. and Weber, S. L.: Climate of the Last Glacial Maximum: sensitivity studies and model-data comparison with the LOVECLIM coupled model, Clim Past, 3(2), 205–224, 2007.

Ruddiman, W. F., Vavrus, S. J. and Kutzbach, J. E.: A test of the overdue-glaciation hypothesis, Quaternary Sci Rev, 24(1-2), 1–10, doi:10.1016/j.quascirev.2004.07.010, 2005.

Russell, J. L., Stouffer, R. J. and Dixon, K. W.: Intercomparison of the Southern Ocean circulations in IPCC coupled model control simulations, J Climate, 19(18), 4560–4575, doi:10.1175/Jcli3869.1, 2006.

Schmittner, A., Latif, M. and Schneider, B.: Model projections of the North Atlantic thermohaline circulation for the 21st century assessed by observations, Geophys. Res. Lett., 32(23), doi:10.1029/2005gl024368, 2005.

Schmittner, A., Silva, T. A. M., Fraedrich, K., Kirk, E. and Lunkeit, F.: Effects of Mountains and Ice Sheets on Global Ocean Circulation, J Climate, 24(11), 2814–2829, doi:10.1175/2010jcli3982.1, 2011a.

Schmittner, A., Urban, N. M., Shakun, J. D., Mahowald, N. M., Clark, P. U., Bartlein, P. J., Mix, A. C. and Rosell-Mele, A.: Climate sensitivity estimated from temperature reconstructions of the Last Glacial Maximum, Science, 334(6061), 1385–1388, doi:10.1126/science.1203513, 2011b.

Semtner, A. J., Jr: A model for the thermodynamic growth of sea ice in numerical investigations of climate, Journal of Physical Oceanography, 1976.

Shakun, J. D., Clark, P. U., He, F., Marcott, S. A., Mix, A. C., Liu, Z., Otto-Bliesner, B. L., Schmittner, A. and Bard, E.: Global warming preceded by increasing carbon dioxide concentrations during the last deglaciation, Nature, 484(7392), 49–54, doi:10.1038/nature10915, 2012.

Singarayer, J. S. and Valdes, P. J.: Quaternary Science Reviews, Quaternary Sci Rev, 29(1-2), 43–55, doi:10.1016/j.quascirev.2009.10.011, 2010.

Sowers, T., Alley, R. B. and Jubenville, J.: Ice core records of atmospheric N2O covering the last 106,000 years, Science, 301(5635), 945–948, 2003.

Srokosz, M., Baringer, M., Bryden, H., Cunningham, S., Delworth, T., Lozier, S., Marotzke, J. and Sutton, R.: Past, Present, and Future Changes in the Atlantic Meridional Overturning Circulation, Bull. Amer. Meteor. Soc., 93(11), 1663–1676, doi:10.1175/bams-d-11-00151.1, 2012.

Tabor, C. R., Poulsen, C. J. and Pollard, D.: Mending Milankovitch's theory: obliquity amplification by surface feedbacks, Clim Past, 10(1), 41–50, doi:10.5194/cp-10-41-2014, 2014.

Thompson, S. L. and Pollard, D.: A Global Climate Model (Genesis) with a Land-Surface Transfer Scheme (Lsx) .1. Present Climate Simulation, J Climate, 8(4), 732–761, 1995.

Thompson, S. L. and Pollard, D.: Greenland and Antarctic mass balances for present and doubled atmospheric CO2 from the GENESIS version-2 global climate model, J Climate, 10(5), 871–900, 1997.

Timm, O. and Timmermann, A.: Simulation of the last 21 000 years using accelerated transient boundary conditions, J Climate, 2007.

Timm, O., Köhler, P., Timmermann, A. and Menviel, L.: Mechanisms for the onset of the African humid period and Sahara greening 14.5–11 ka BP, J Climate, 23(10), 2612–2633, doi:10.1175/2010jcli3217.1, 2010.

Timm, O., Timmermann, A., Abe-Ouchi, A., Saito, F. and Segawa, T.: On the definition of seasons in paleoclimate simulations with orbital forcing, Paleoceanography, 23(2), doi:10.1029/2007PA001461, 2008.

Unterman, M. B., Crowley, T. J., Hodges, K. I., Kim, S. J. and Erickson, D. J.: Paleometeorology: High resolution Northern Hemisphere wintertime mid-latitude dynamics during the Last Glacial Maximum, Geophys. Res. Lett., 38(23), L23702, doi:10.1029/2011gl049599, 2011.

Waelbroeck, C., Paul, A., Kucera, M., Rosell-Mele, A., Weinelt, M., Schneider, R., Mix, A. C., Abelmann, A., Armand, L., Bard, E., Barker, S., Barrows, T. T., Benway, H., Cacho, I., Chen, M. T., Cortijo, E., Crosta, X., de Vernal, A., Dokken, T., Duprat, J., Elderfield, H., Eynaud, F., Gersonde, R., Hayes, A., Henry, M., Hillaire-Marcel, C., Huang, C. C., Jansen, E., Juggins, S., Kallel, N., Kiefer, T., Kienast, M., Labeyrie, L., Leclaire, H., Londeix, L., Mangin, S., Matthiessen, J., Marret, F., Meland, M., Morey, A. E., Mulitza, S., Pflaumann, U., Pisias, N. G., Radi, T., Rochon, A., Rohling, E. J., Sbaffi, L., Schaefer-Neth, C., Solignac, S., Spero, H., Tachikawa, K., Turon, J. L. and Members, M. P.: Constraints on the magnitude and patterns of ocean cooling at the Last Glacial Maximum, Nature Geoscience, 2(2), 127–132, doi:10.1038/NGEO411, 2009.

Weber, S. L., Drijfhout, S. S., Abe-Ouchi, A., Crucifix, M., Eby, M., Ganopolski, A., Murakami, S., Otto-Bliesner, B. L. and Peltier, W. R.: The modern and glacial overturning circulation in the Atlantic Ocean in PMIP coupled model simulations, Clim Past, 3(1), 51–64, 2007.

Zhao, Y. and Harrison, S. P.: Mid-Holocene monsoons: a multi-model analysis of the inter-hemispheric differences in the responses to orbital forcing and ocean feedbacks, Clim Dynam, 39(6), 1457–1487, doi:10.1007/s00382-011-1193-z, 2012.

Zheng, W. and Braconnot, P.: Characterization of Model Spread in PMIP2 Mid-Holocene Simulations of the African Monsoon, J Climate, 26(4), 1192–1210, doi:10.1175/JCLI-D-12-00071.1, 2013.

Zhou, J., Poulsen, C. J., Pollard, D. and White, T. S.: Simulation of modern and middle Cretaceous marine delta O-18 with an ocean-atmosphere general circulation model, Paleoceanography, 23(3), doi:10.1029/2008pa001596, 2008.

Table 1. Atmospheric greenhouse gas concentrations for each time slice simulation. The 21 ka through 3 ka values for CO_2 (Monnin et al., 2001), CH_4 (Brook et al., 2000) and N_2O (Sowers et al., 2003) are estimated from ice core records by averaging the gas concentrations within a ± 300 yr window centered at the time of interest. For comparison, the PMIP3 concentrations for 6 ka are 280 ppmV, 650 ppbV, and 270 ppbV for CO_2, CH_4 and N_2O respectively, and 185 ppmV, 350 ppbV, and 200 ppbV for 21 ka. In the table, e is eccentricity, ω-180 is precession and ε is obliquity (Berger and Loutre, 1991).

Jay Alder 12/8/14 1:48 PM
Deleted: -segment

	CO_2 (ppmV)	CH_4 (ppbV)	N_2O (ppbV)	e	ω-180	ε
PD	355	1714	311	0.0176	101.37	23.446
PI	280	760	270	0.0176	101.37	23.446
3 ka	275	627	264	0.0183	50.30	23.815
6 ka	260	596	227	0.0192	0.01	24.100
9 ka	260	677	244	0.0198	310.32	24.229
12 ka	240	500	246	0.0201	261.07	24.161
15 ka	220	500	216	0.0202	212.04	23.895
18 ka	188	382	219	0.0199	163.04	23.475
21 ka	188	392	199	0.0194	113.98	22.989

Table 2. Annual average 2-m air temperatures and precipitation rates for the time slice simulations. NCEP is from the National Center for Environmental Predication NCEP/NCAR Reanalysis data set (Kalnay et al., 1996), PD2X is the 2xCO_2 simulation, PD is present day and PI is pre-industrial. Parenthetical values are the changes from the previous time slice, e.g., the global average temperature for the PD is 0.77 °C warmer than the PI.

Jay Alder 12/8/14 1:49 PM
Deleted: segment

Jay Alder 12/8/14 1:49 PM
Deleted: segment

	Temperature (K)			Precipitation (mm d^{-1})		
	Global	Land	Ocean	Global	Land	Ocean
NCEP (1980-2000)	287.52 --	281.66 --	289.84 --	3.09 --	2.30 --	3.40 --
PD2X	288.48 (2.2)	282.06 (2.69)	291.29 (1.91)	3.11 (0.11)	2.17 (0.10)	3.53 (0.13)
PD	286.34 (0.77)	279.37 (0.93)	289.38 (0.70)	3.00 (0.04)	2.07 (0.04)	3.40 (0.05)
PI	285.57 (0.07)	278.44 (-0.03)	288.68 (0.15)	2.95 (0.00)	2.03 (-0.02)	3.36 (0.02)
3 ka	285.50 (0.32)	278.47 (0.30)	288.53 (0.33)	2.95 (0.02)	2.05 (0.00)	3.34 (0.04)
6 ka	285.17 (0.23)	278.18 (0.95)	288.20 (-0.27)	2.93 (0.02)	2.05 (0.00)	3.30 (0.02)
9 ka	284.95 (0.74)	277.23 (1.63)	288.47 (0.22)	2.91 (0.05)	2.05 (0.06)	3.30 (0.03)
12 ka	284.21 (1.40)	275.60 (2.44)	288.25 (0.70)	2.86 (0.09)	1.99 (0.12)	3.26 (0.05)
15 ka	282.81 (0.93)	273.16 (1.53)	287.55 (0.53)	2.77 (0.05)	1.87 (0.09)	3.21 (0.02)
18 ka	281.88 (0.16)	271.63 (0.28)	287.02 (0.06)	2.72 (0.01)	1.78 (0.01)	3.19 (0.01)
21 ka	281.72	271.35	286.96	2.71	1.78	3.18

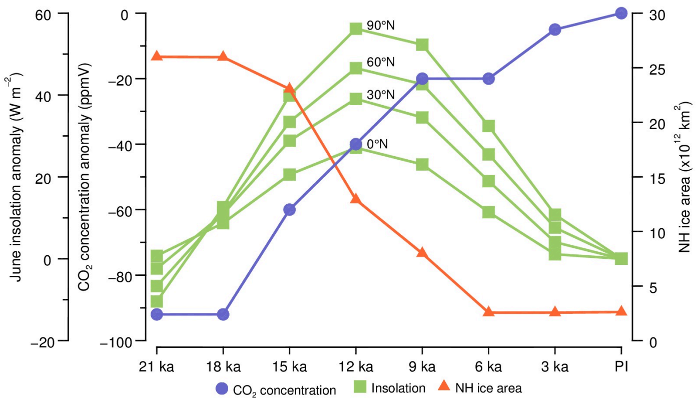

Fig. 1. Boundary conditions for the time slice simulations. CO_2 concentrations are relative to the PI concentration of 280 ppmV. NH ice area is the total area covered by the continental ice sheets. June insolation anomalies are relative to PI at the indicated latitude. Mid-month insolation data from Berger and Loutre (1991).

Jay Alder 12/8/14 1:49 PM
Deleted: -segment

Jay Alder 12/11/14 10:24 AM
Deleted: Insolation

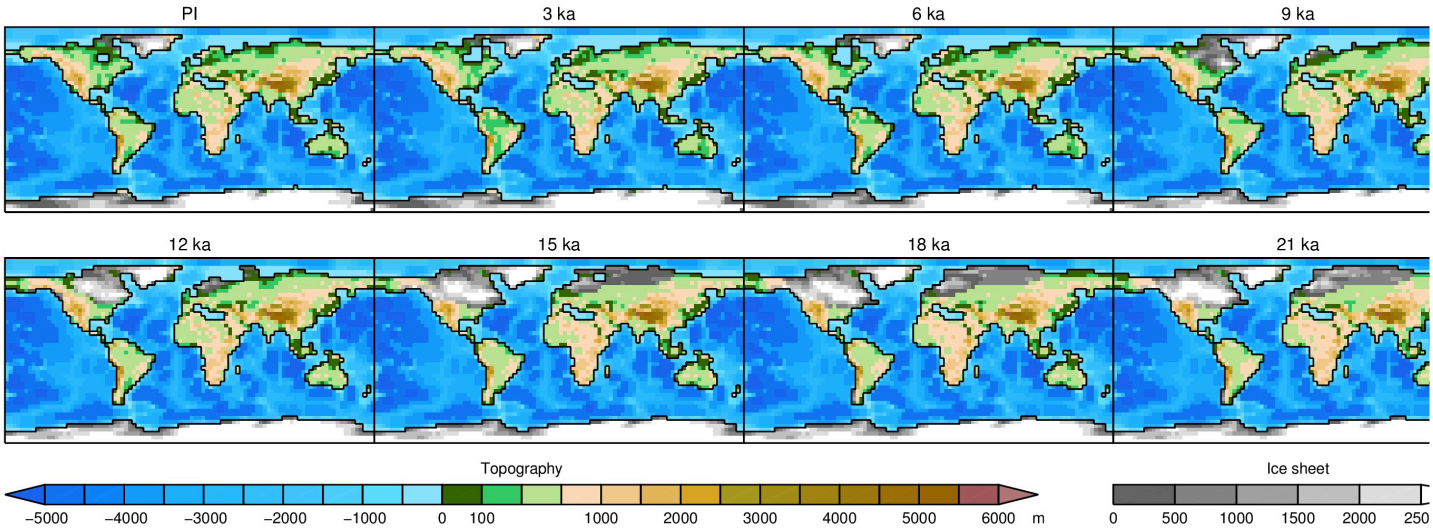

Fig. 2. Orography for the time slice simulations, with ice sheet height and extent derived from ICE-4G (Peltier, 2002) for the Fennoscandian, Cordilleran and Antarctic, and OSU-LIS (Licciardi et al., 1998) for the Laurentide.

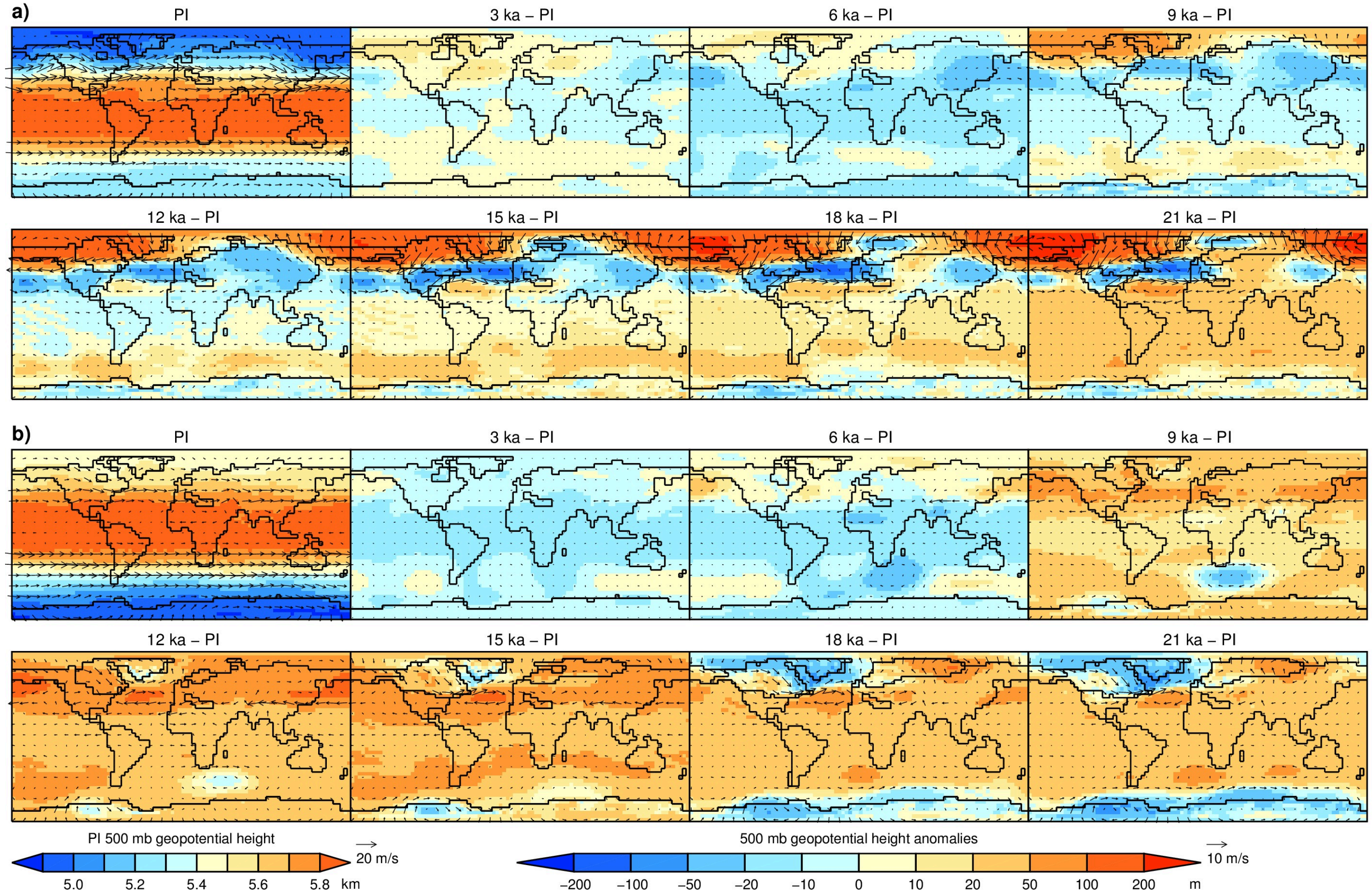

Fig. 3. Simulated seasonal 500 hPa geopotential height and wind anomalies relative to PI. a) December, January, and February and b) June, July and August. Raw 500 hPa geopotential height and wind are shown in SFig. 2.

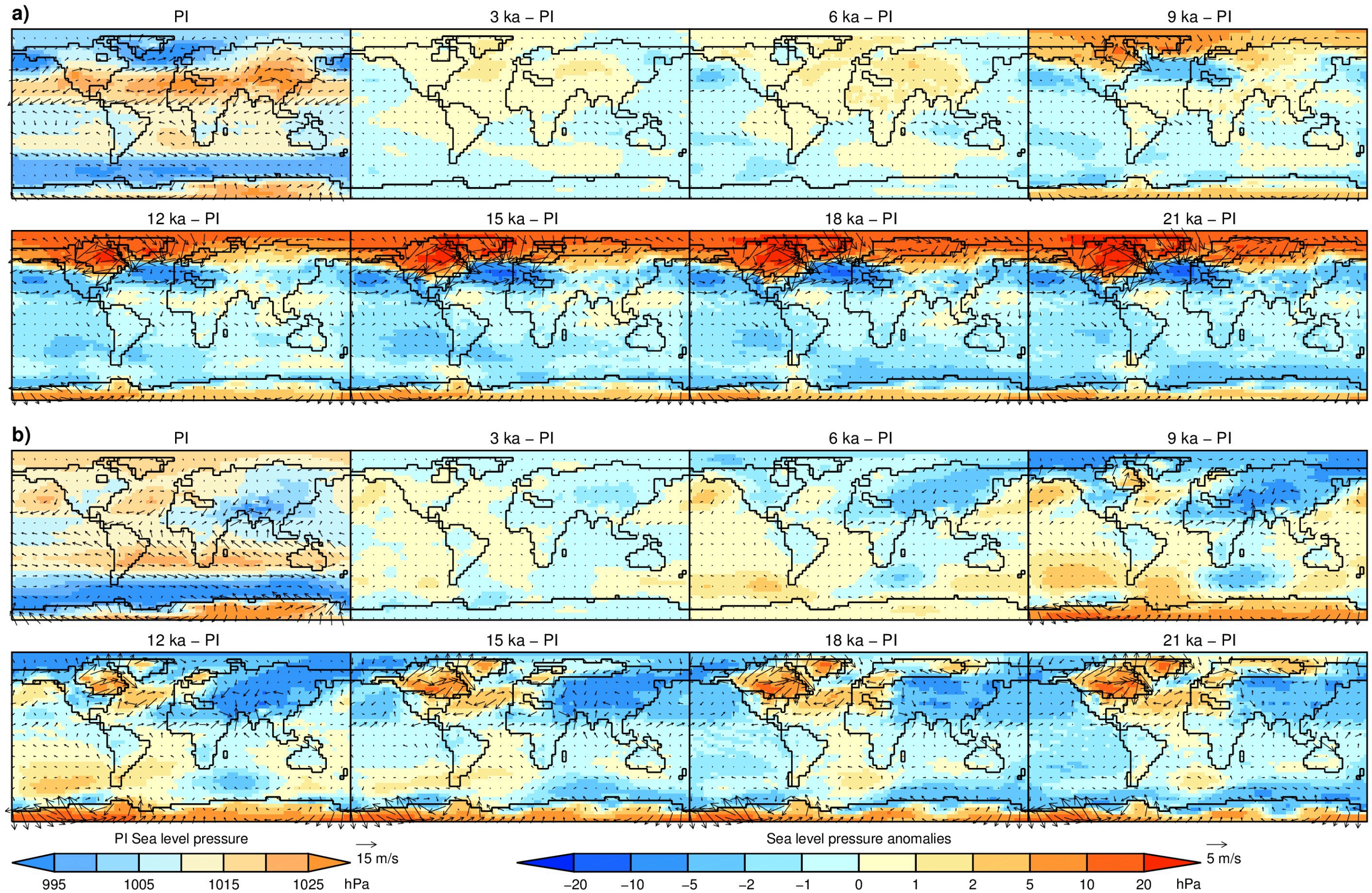

Fig. 4. Simulated seasonal average sea-level pressure and 2-m wind anomalies relative to PI. a) December, January, and February and b) June, July, and August. Raw sea level pressure and wind are shown in SFig. 3.

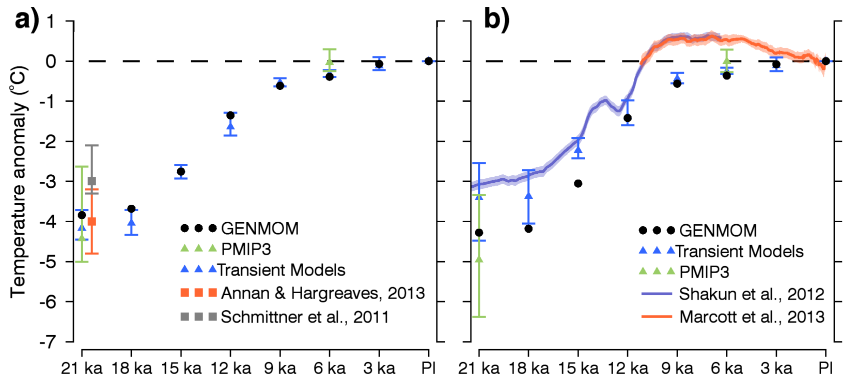

Fig. 5. Simulated and reconstructed changes in temperature from 21 ka to present. a) Global mean surface air temperature from GENMOM compared to the PMIP3 ensemble average and three transient models (CCSM {Liu:2009jv}, LOVECLIM {Timm:2007ii} and FAMOUS {Smith:2012iq}). The transient model values are averages over a ±50 yr window centered on the eight time slices. The symbols for the PMIP and transient models are the average of the ensembles and the bars represent the range of the ensembles. Data-model estimates of mean and range of LGM cooling by Annan and Hargreaves (2013) and Schmittner et al. (2011b) are offset from 21 ka for legibility. b) Temperature change at the proxy sites used in the reconstructions by Shakun et al. (2012) and Marcott et al (2013). The models were bilinearly interpolated and aggregated to the 5° x 5° boxes around the proxy sites as in Marcott et al. (2013).

Steve 1/16/15 9:41 AM
Deleted: Changes Global sin surface air temperature (SAT)

Jay Alder 12/12/14 1:54 PM
Deleted: changes

Steve 1/16/15 9:30 AM
Deleted: The g

Steve 1/16/15 9:30 AM
Deleted: change in

Steve 1/16/15 9:30 AM
Deleted: is

Steve 1/16/15 9:41 AM
Deleted: :

Steve 1/16/15 9:31 AM
Deleted: temporal resolution is degraded to that of GENMOM by

Steve 1/16/15 9:31 AM
Deleted: ing

Steve 1/16/15 9:42 AM
Deleted:

Steve 1/16/15 9:42 AM
Deleted: ear

Steve 1/16/15 9:32 AM
Deleted: around

Jay Alder 12/12/14 2:03 PM
Deleted: is shown as 100-yr averages and standard deviations.

Steve 1/16/15 9:33 AM
Deleted: Both PMIP3 and transient model error bars represent

Steve 1/16/15 9:45 AM
Deleted: min/max of

Jay Alder 12/12/14 2:04 PM
Deleted: The 21 ka and 6 ka PMIP3 data are shown as the ensemble average and its standard deviation.

Steve 1/16/15 9:34 AM
Deleted: (

Steve 1/16/15 9:34 AM
Deleted:)

Jay Alder 12/12/14 2:05 PM
Deleted: Annan and Hargreaves (2013) and Schmittner et al. (2011b) are offset from 21 ka for legibility.

Steve 1/16/15 9:47 AM
Deleted: sampled

Steve 1/16/15 9:35 AM
Deleted: . R

The 1σ uncertainty in the reconstructions is indicated by the shaded band. Marcott et al. (2013) is adjusted to a pre-industrial (~1850) base value rather than the original 1961-1990. Data younger than pre-industrial are removed. The Shakun et al. (2012) and Marcott et al. (2013) time series are joined at their 11.5 ka – 6.5 ka means.

Steve 1/16/15 9:35 AM
Deleted: display 1σ uncertainty as

Steve 1/16/15 9:36 AM
Deleted: a

Jay Alder 12/12/14 2:18 PM
Deleted: were

Steve 1/16/15 9:36 AM
Deleted: Each of the models are bilinearly interpolated to the Marcott et al. (2013) proxy sites and aggregated to a 5° x 5° box.

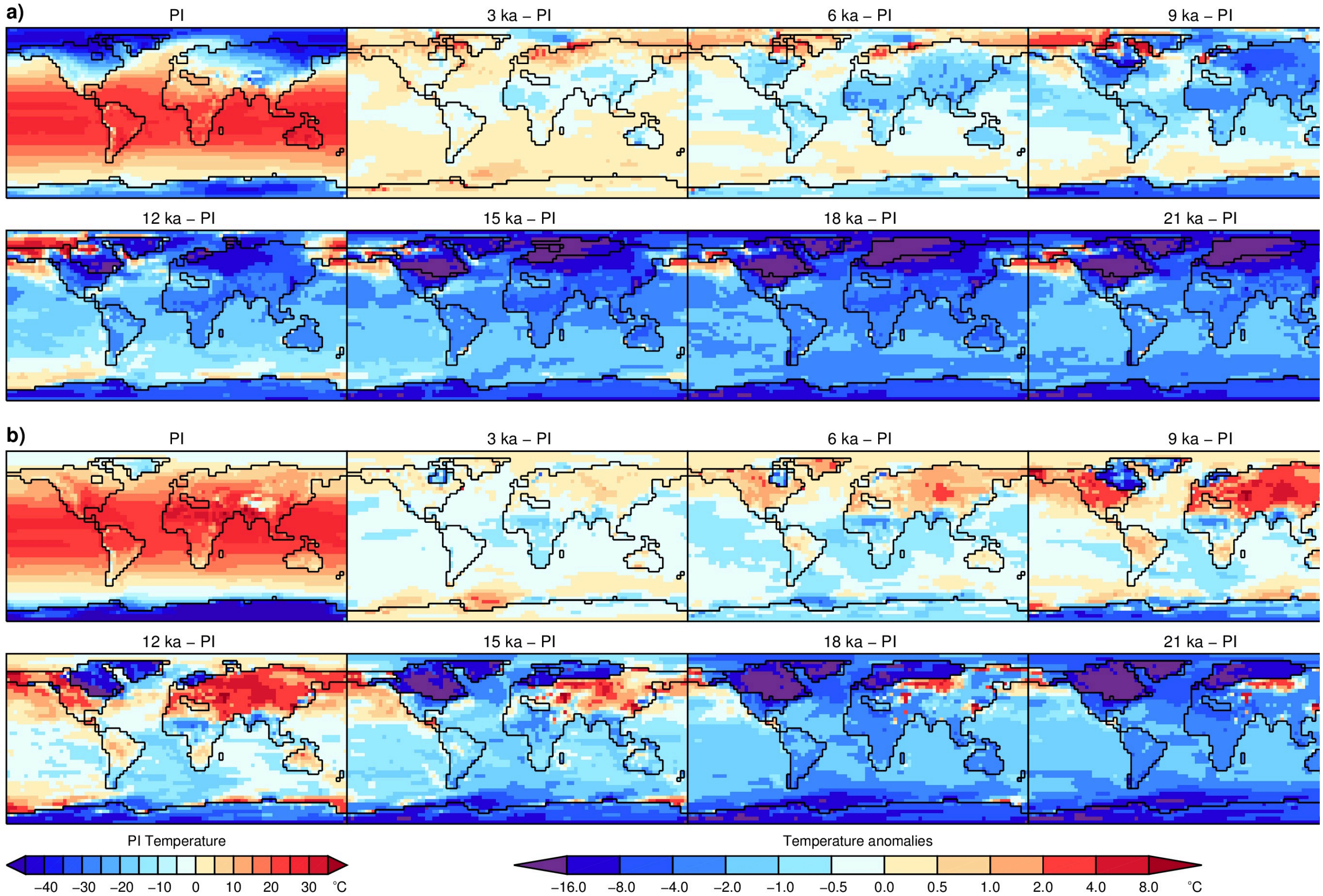

1173
1174 Fig. 6. Simulated seasonal average 2-m air temperature anomalies relative to PI. a) December, January, and February and b) June,
1175 July, and August.

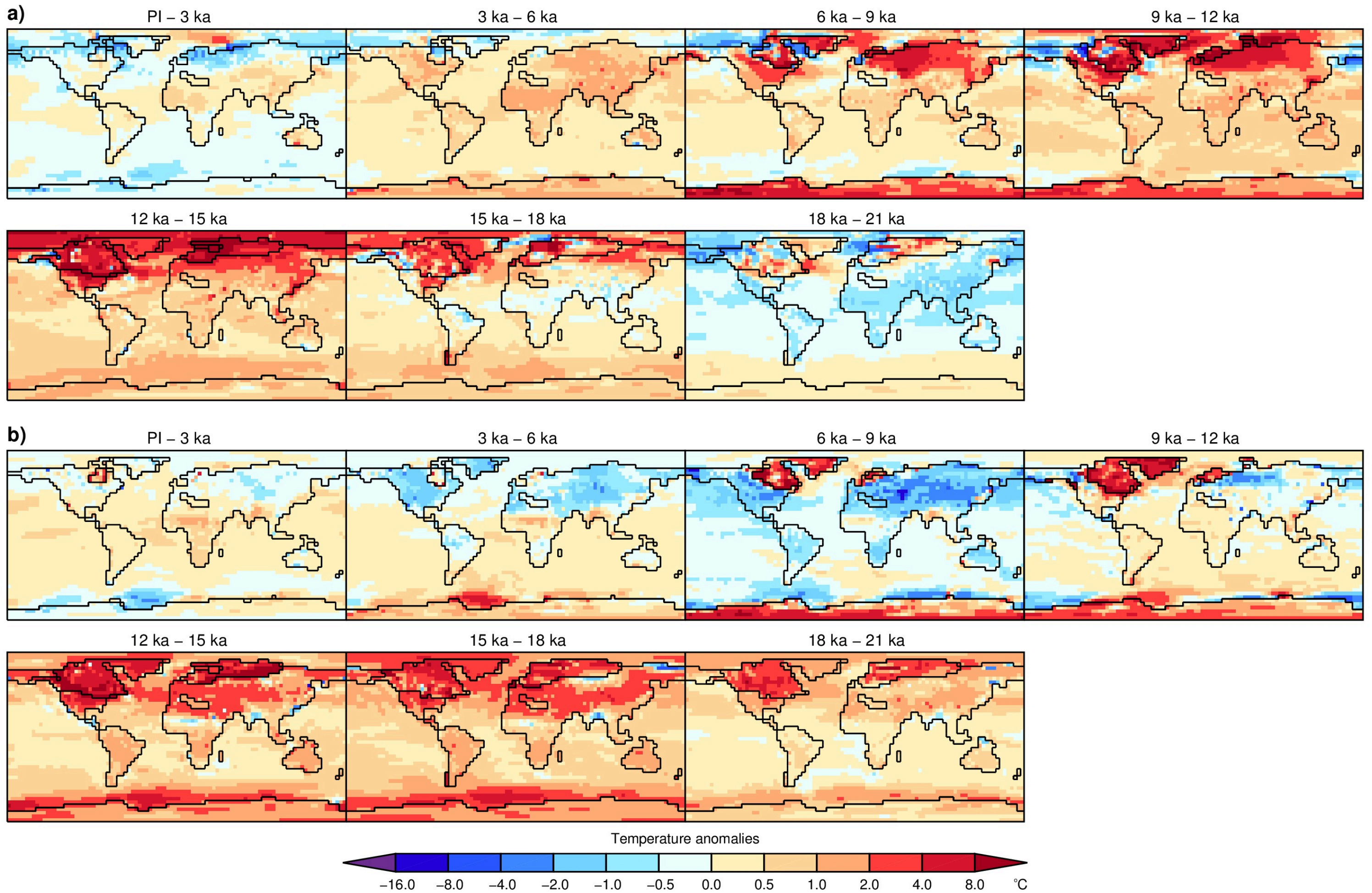

Fig. 7. Simulated seasonal average changes in 2-m air between consecutive time slices, a) December, January, and February and b) June, July, and August.

Jay Alder 12/8/14 1:49 PM
Deleted: segments

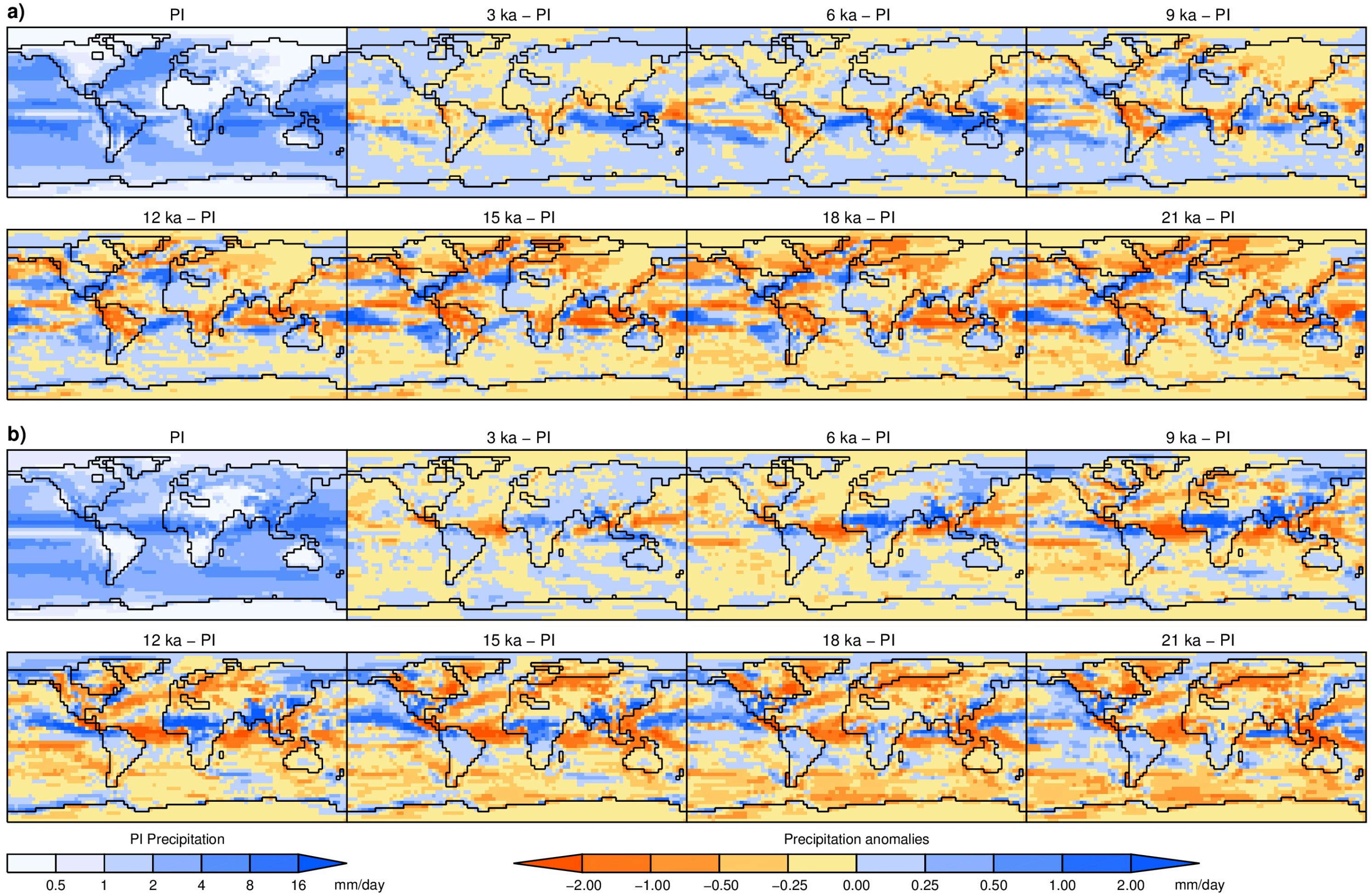

Fig. 8. Simulated seasonal average precipitation anomalies relative to PI. a) December, January, and February and b) June, July, and August.

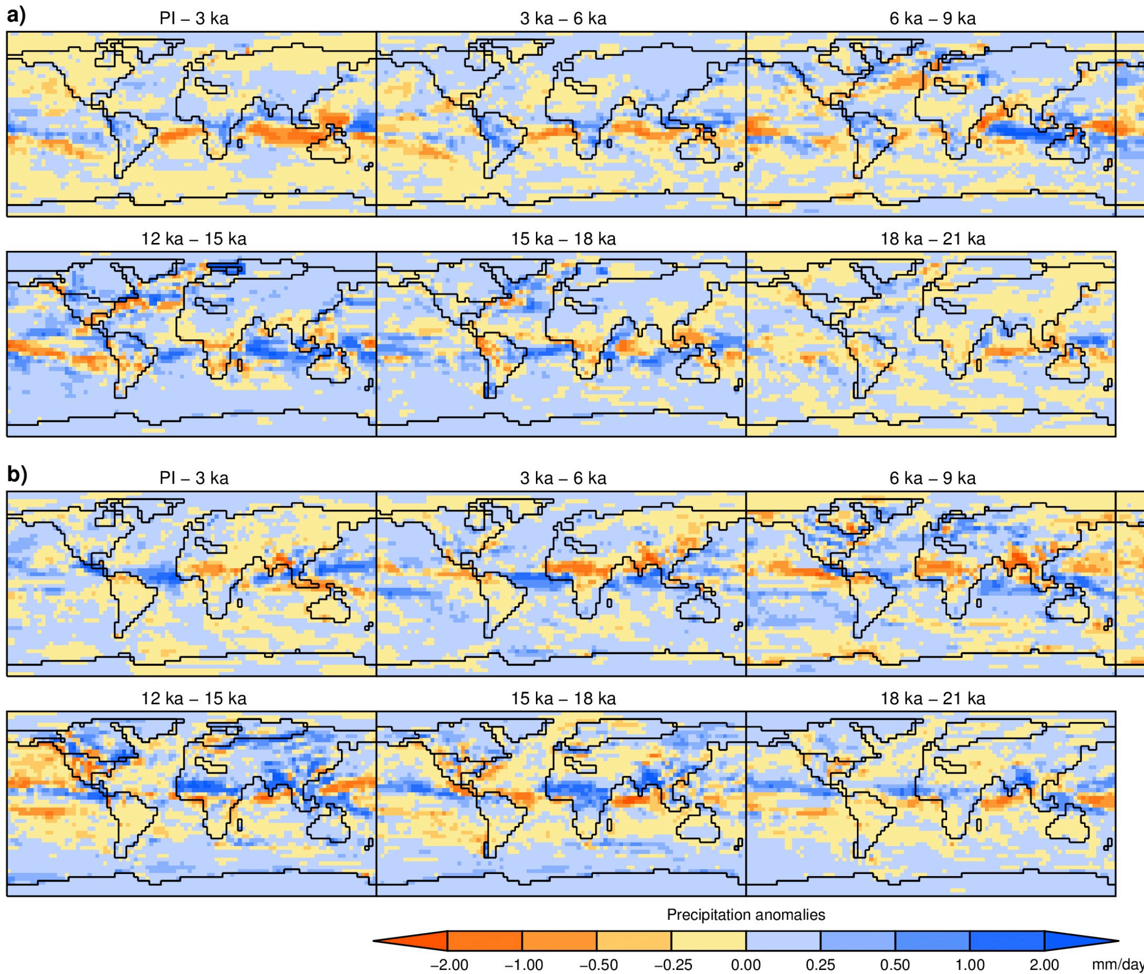

Fig. 9. Simulated seasonal average precipitation changes between consecutive time slices, a) December, January, and February and b) June, July, and August.

Jay Alder 12/8/14 1:49 PM
Deleted: segments

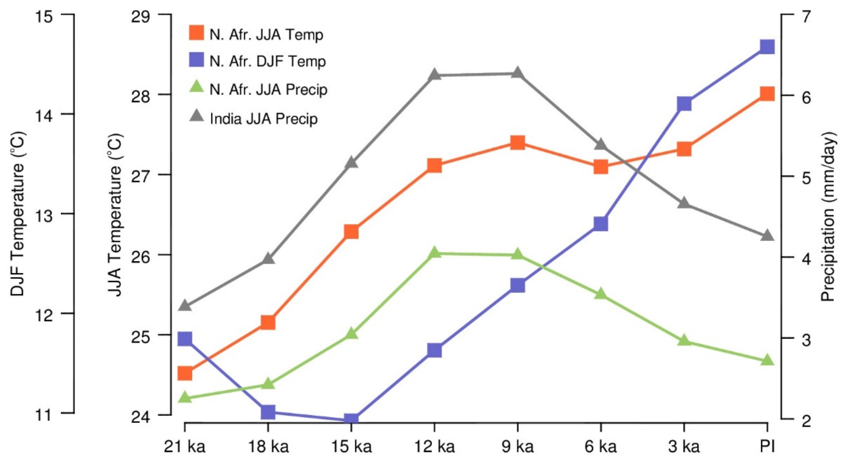

Fig. 10. Time evolution of North African and Indian summer monsoons. The North Africa monsoon region is defined as 12°N - 30°N, 20°W - 30°E and India monsoon region is defined as 20°N - 40°N, 70°E - 100°E (Zhao and Harrison, 2012).

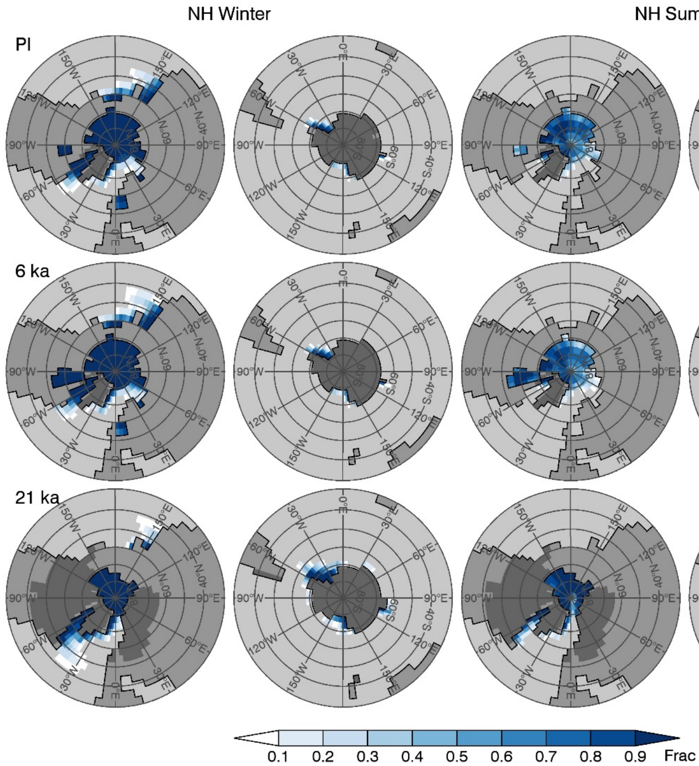

Fig. 11 Simulated sea-ice fraction for PI, 6 ka and 21 ka. Left two columns: February-March and right two columns: August-September. Medium gray is continental land mass and dark gray is continental ice sheet.

Unknown
Deleted: 21 ka, 6 ka and PI

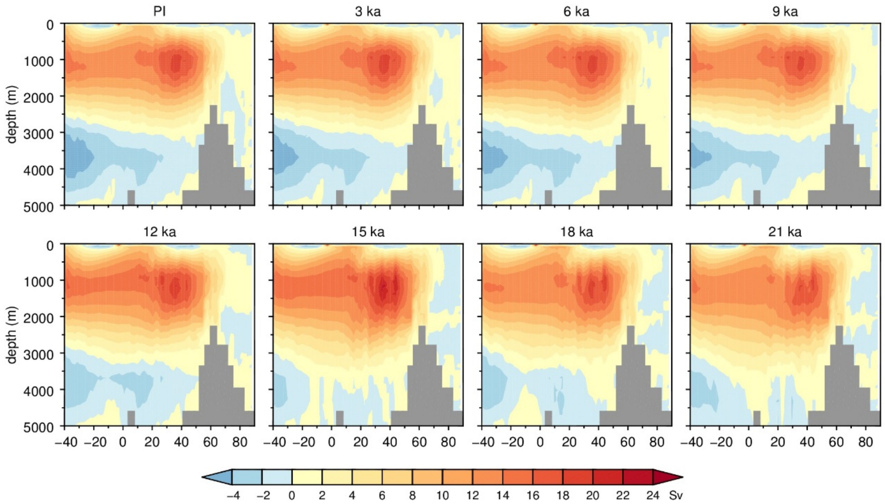

Fig. 12. Simulated annual average Atlantic Meridional Overturning Circulation (AMOC) for the eight time-slices.

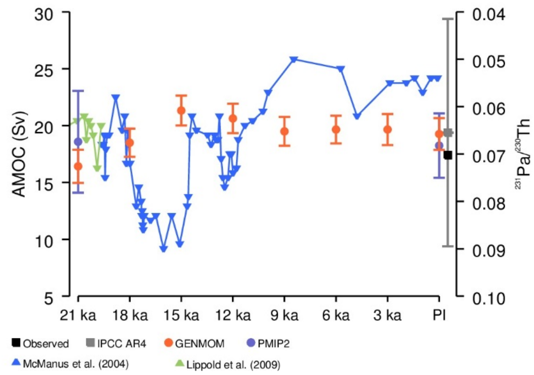

Fig. 13. Simulated Atlantic Meridional Overturning Circulation (AMOC) compared to $^{231}Pa/^{230}Th$ proxy record at 33°N and other AOGCMs. Observations are from 26.5°N. GENMOM values are 100-yr averages with error bars representing standard deviations. The mean and standard deviation of the maximum AMOC in the five PMIP2 models. The IPCC AR4 point represents the mean and standard deviation from a collection of IPCC AR4 models. $^{231}Pa/^{230}Th$ data from McManus et al. (2004) and Lippold et al. (2009); observed value from Srokosz et al. (2012), PMIP2 data from Weber et al. (2007), and IPCC data from Schmittner et al. (2005).

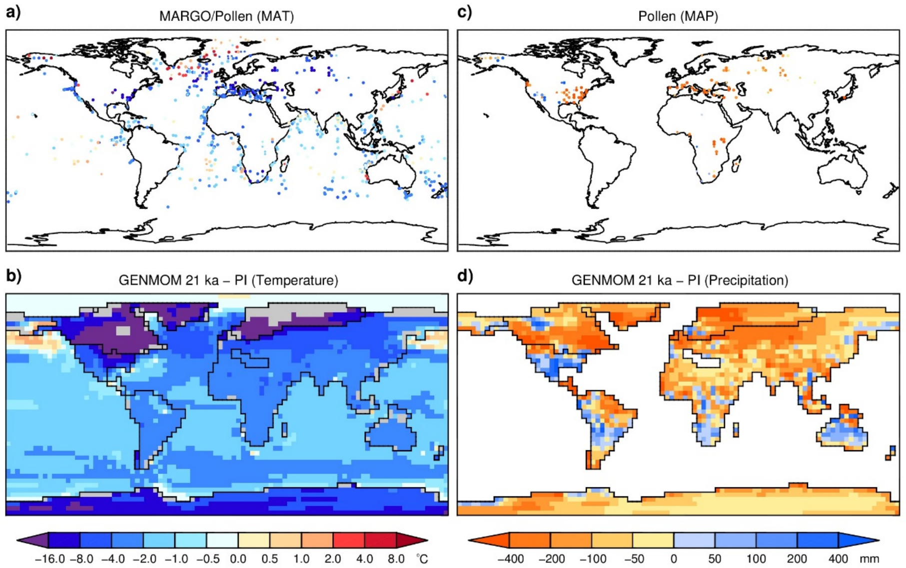

Fig. 14. Changes in 21 ka mean annual temperature (MAT) and precipitation (MAP) inferred from data and simulated by GENMOM. a) blended sea surface temperature from MARGO (Waelbroeck et al., 2009) and terrestrial temperature from Bartlein et al. (2011), b) GENMOM temperature anomalies (blended sea surface temperature and 2-m air temperature over land), c) precipitation from Bartlein et al. (2011), and d) GENMOM precipitation anomalies. Grid cells with different land mask types in the 21 ka and PI simulation are shaded in gray to avoid comparing ocean temperature to land temperature in emergent cells.

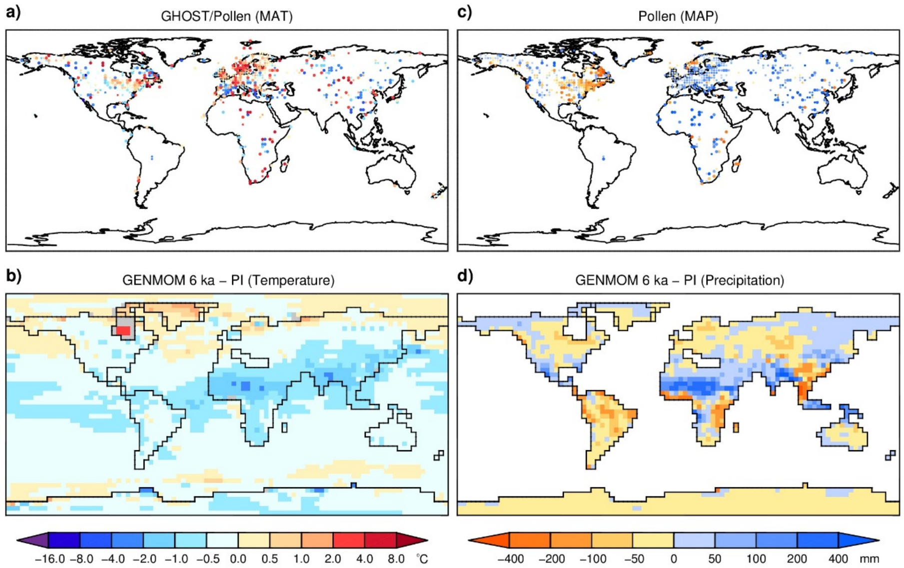

Fig. 15. Changes in 6 ka mean annual temperature (MAT) and precipitation (MAP) inferred from data and simulated by GENMOM. a) blended sea surface temperature from Leduc et al. (2010) and terrestrial temperature from Bartlein et al. (2011), b) GENMOM temperature anomalies (blended sea surface temperature and 2-m air temperature over land), c) precipitation from Bartlein et al. (2011) and d) GENMOM precipitation anomalies. Grid cells with different land mask types in the 6 ka and PI simulation are shaded in gray to avoid comparing ocean temperature to land temperature in emergent cells.